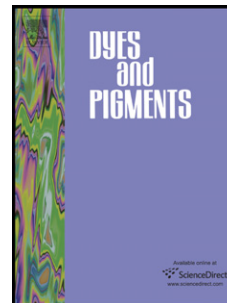


Accepted Manuscript

Synthesis, photophysical and electrochemical properties of aza-boron-diquinomethene complexes

Danfeng Wang, Rui Liu, Chen Chen, Shifan Wang, Jin Chang, Chunhui Wu, Hongjun Zhu, Eric R. Waclawik



PII: S0143-7208(13)00174-5

DOI: [10.1016/j.dyepig.2013.05.009](https://doi.org/10.1016/j.dyepig.2013.05.009)

Reference: DYPI 3946

To appear in: *Dyes and Pigments*

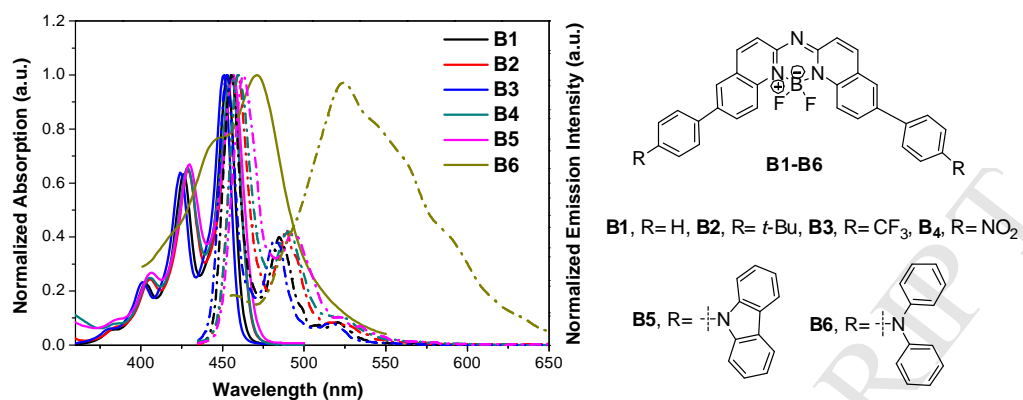
Received Date: 26 March 2013

Revised Date: 3 May 2013

Accepted Date: 11 May 2013

Please cite this article as: Wang D, Liu R, Chen C, Wang S, Chang J, Wu C, Zhu H, Waclawik ER, Synthesis, photophysical and electrochemical properties of aza-boron-diquinomethene complexes, *Dyes and Pigments* (2013), doi: 10.1016/j.dyepig.2013.05.009.

This is a PDF file of an unedited manuscript that has been accepted for publication. As a service to our customers we are providing this early version of the manuscript. The manuscript will undergo copyediting, typesetting, and review of the resulting proof before it is published in its final form. Please note that during the production process errors may be discovered which could affect the content, and all legal disclaimers that apply to the journal pertain.



Abstract: A series of aza-boron-diquinomethene complexes **B1-B6** exhibit sharp absorption and emission bands with high photoluminescence quantum yields ($\Phi_{\text{PL}} = 0.47 - 0.93$).

Highlights

Our work succeeds in synthesizing a series of aza-boron-diquinomethene complexes.

These complexes show high fluorescence quantum yields and thermal stability.

Optical, electrochemical properties and DFT calculations were investigated.

These complexes are expected to be promising light-emitting materials in OLEDs.

Synthesis, photophysical and electrochemical properties of
aza-boron-diquinomethene complexes

Danfeng Wang^a, Rui Liu^a, Chen Chen^a, Shifan Wang^a, Jin Chang^b, Chunhui Wu^a,
Hongjun Zhu^{a*}, Eric R. Waclawik^b

^a *Department of Applied Chemistry, College of Science, Nanjing University of
Technology, Nanjing 210009, P. R. China*

^b *Discipline of Chemistry, Queensland University of Technology, 2 George St.,
Brisbane 4000, Australia*

*Corresponding author. Phone: +86-25-83172358. Fax: +86-25-83587428. E-mail:

zhuhj@njut.edu.cn

ABSTRACT

A series of aza-boron-diquinomethene (aza-BODIQU) complexes with different aryl-substituents (**B1-B6**) were synthesized and characterized. Their photophysical properties were investigated systematically via spectroscopic and theoretical methods. All complexes exhibit strong ${}^1\pi\text{-}\pi^*$ absorption bands and intense fluorescent emission bands in the visible spectral region at room temperature. The fluorescence spectra in solution show the mirror image features of the $S_0\rightarrow S_1$ absorption bands, which can be assigned to the ${}^1\pi\text{-}\pi^*/{}^1\text{ICT}$ (intramolecular charge transfer) emitting states. Except for **B6**, all complexes exhibit high photoluminescence quantum yields ($\Phi_{\text{PL}} = 0.47\text{-}0.93$). The spectroscopic studies and theoretical calculations indicate that the photophysical properties of these aza-BODIQUs can be tuned by the appended aryl-substituents, which would be useful for rational design of boron-fluorine complexes with high emission quantum yield for organic light-emitting applications.

Keywords:

Fluorescence; Synthesis; Optical properties; Electrochemical properties; Boron-fluorine complexes; DFT calculations.

1. Introduction

Boron dipyrromethene (BODIPY) complexes have attracted great interest in the past two decades due to their potential applications in molecular probes, photodynamic therapy, laser dyes, nonlinear optical materials and solar cells [1]. These various applications are intrinsically based on their rich photophysical properties, such as strong ground-state absorption, intense fluorescent emission, high photoluminescence quantum yield and high chemical stability. In addition, their photophysical properties can be readily tuned by structural modifications, which provide additional opportunities to meet the different requirements for diverse applications.

In the past decade, the core structure of BODIPY has been modified and developed into its aza-derivatives, such as aza-boron-dipyrromethene, aza-boron-diindolmethene, aza-boron-dipyridomethene, aza-boron-diquinomethene, *ect.*, as shown in Scheme 1 [2]. These complexes exhibit high photoluminescence quantum yields, good electron-transporting property and excellent thermal stability, which could be utilized in organic light emitting devices (OLEDs) [3,4]. Compared to the traditional BODIPYs, the pyridoamine-based BODIPY were first synthesized by Boyer and co-workers in 1993 [5], and then photophysically investigated by Jorge Bañuelos and co-workers in 2011 [6]. In many cases, the quinoline-based compounds show better electron mobility than pyrrole and pyridine derivatives [7], suggesting that quinoline structure is also a good candidate in the construction of boron-fluorine complexes. Recently, Kondakova and co-workers reported an aza-boron-diquinomethene complex, which was utilized as a deep blue fluorescent emitting material in the fabrication of white OLEDs ($\eta_{p,1000} =$

30 lm W⁻¹) [8]. Although the results are intriguing, the investigation on the aza-boron-diquinomethene is still limited. In order to improve the optical properties by structural modification, understanding the structure-property correlation becomes critical. Taking all these factors into consideration, the development of new BF₂ complexes, the investigation of their photophysical properties and structure-property relationships are still feasible, challengeable and potentially valuable.

In this work, we designed and synthesized a series of new BF₂ complexes with different aryl-substituents on the core structure. The synthetic routes and the structures of the target complexes are displayed in Scheme 2. The *t*-Bu, -NPh₂ and carbazolyl groups were chosen as the electron-donating substituent and the NO₂ and CF₃ groups were chosen as electron-withdrawing substituents. The photophysical and electrochemical properties of these complexes were systematically investigated with the aim of understanding the structure-property correlations and developing novel blue light-emitting materials. Furthermore, a novel and versatile synthesis procedure for symmetrical *N*-arylation of heteroarylamines with high efficiency and selectivity was also developed.

2. Experimental section

2.1. Materials

All solvents and reagents for synthesis were purchased from Aldrich, TCI and Sinopharm Chemical Regent Co. Ltd. and used as is unless otherwise stated. Tetrahydrofuran (THF), toluene and *N,N*-diisopropylethylamine (DIEA) were distilled

under N₂ over sodium benzophenone ketyl. Tetra-*n*-butylammonium perchlorate (TBAP) and ferrocene were purified by recrystallization twice from ethanol. The related boronic acids were synthesized according to the literature procedures [9]. Silica gel (200-300 mesh) used for chromatography was purchased from Sinopharm Chemical Reagent Co. Ltd.

2.2. Measurements

¹H NMR and ¹³C NMR spectra were recorded on a Bruker 300 MHz or 400 MHz spectrometer using DMSO-*d*₆ or CDCl₃ as the solvent. Chemical shifts were referred to the internal standard tetramethylsilane (TMS). ¹⁹F NMR spectra were recorded at room temperature with CFCl₃ as internal standard at 376 MHz. Melting points (m.p.) were taken on an X-4 microscope electrothermal apparatus (Taiké China). The elemental analyses were performed with a Vario El III elemental analyzer. Mass spectra were obtained on a VG12-250 mass spectrometer and an Agilent 1100 mass spectrometer. UV-Vis spectra were recorded using an HP-8453 UV/Vis/near-IR spectrophotometer (Agilent) with a 1 cm quartz cell. Photoluminescence spectra were carried out on a LS-55 spectrofluorometer (Perkin-Elmer). Photoluminescence quantum yields were carried out on a LFS920 spectrofluorometer (Edinburgh). Electrochemical experiments were carried out using a CHI 660C electrochemistry workstation (CHI-USA). A standard one-compartment three-electrode cell was used with a Pt electrode as the working electrode, a Pt wire as the counter electrode and an Ag/AgNO₃ electrode (Ag in 0.1 M AgNO₃ solution) as the reference electrode. TBAP (0.1 M) was used as the

supporting electrolyte. The scan rate was 100 mV S^{-1} . Differential scanning calorimetry (DSC) was conducted on a DSC instruments (NETZSCH DSC 204).

2.3. DFT calculations

Quantum chemical calculations were performed for complexes **B1-B6**, in order to understand the nature of the ground state and the low-lying excited states. All calculations were conducted at the DFT level of theory, in conjunction with the B3LYP functional [10] and the 6-31G* basis set [11], as implemented in the Gaussian 09 program package [12]. In this work, geometry optimization and the frontier molecular orbitals were simulated for each of the compound.

2.4. Synthesis

2.4.1. Synthesis of 6-bromoquinoline (**1**)

Glycerol (60.0 mL, 0.82 mol), $\text{FeSO}_4 \cdot 7\text{H}_2\text{O}$ (7.00 g, 0.025 mol), *p*-bromoaniline (34.40 g, 0.20 mol), and nitrobenzene (12.5 mL, 0.13 mol) were added to a three-necked round bottom flask with mechanical stirring. H_2SO_4 (35.0 mL, 0.64 mol) was added to the system slowly while kept the temperature below $100 \text{ }^\circ\text{C}$. The mixture was then heated to reflux for 20 h. After cooling to r.t., adjusted pH to 7 with 50% NaOH aq. solution and extracted with diethyl ether. The extraction was dried over MgSO_4 and concentrated in vacuo. The product was isolated by reduced pressure distillation. Fraction was collected at $138\text{-}140 \text{ }^\circ\text{C}$, 16 torr (lit. [13] $161\text{-}162 \text{ }^\circ\text{C}$, 22 Torr). Light yellow liquid was afforded (11.90 g, 28.6% yield). ^1H NMR (300 MHz,

DMSO- d_6) δ (ppm): 9.00 (d, $J = 4.1$ Hz, 1H), 8.37 (d, $J = 8.3$ Hz, 1H), 8.28 (d, $J = 1.7$ Hz, 1H), 8.02 (d, $J = 9.2$ Hz, 1H), 7.89 (dd, $J_1 = 9.0$ Hz, $J_2 = 2.1$ Hz, 1H), 7.62 (q, $J = 8.3$ Hz, 1H)

2.4.2. Synthesis of 6-bromoquinoline *N*-oxide (**2**)

m-chloroperoxybenzoic acid (*m*-CPBA) (5.07 g, 29.4 mmol) was added slowly to a CH_2Cl_2 solution of **1** (6.00 g, 26.7 mmol) at r.t., then stirred overnight. The reaction was filtered and the filtrate was treated with saturated NaHCO_3 solution until no CO_2 gas yield. Then, adjusted pH = 10 with 3 N NaOH aq. solution and extracted with CH_2Cl_2 50 mL three times. The solvent was removed under reduced pressure. The crude product was then purified by silica gel column chromatography (2% methanol/ CH_2Cl_2). Pale yellow solid was afforded (4.00 g, 66.9% yield), m.p. 137-139 °C (lit. [14] 140-142 °C). ^1H NMR (400 MHz, CDCl_3) δ (ppm): 8.63 (d, $J = 9.3$ Hz, 1H), 8.55 (d, $J = 6.0$ Hz, 1H), 8.05 (d, $J = 1.9$ Hz, 1H), 7.83 (dd, $J_1 = 9.3$ Hz, $J_2 = 2.0$ Hz, 1H), 7.67 (d, $J = 8.5$ Hz, 1H), 7.34 (dd, $J_1 = 8.5$ Hz, $J_2 = 6.0$ Hz, 1H).

2.4.3. Synthesis of 2,6-dibromoquinoline (**3**)

To a round bottom flask was charged 6-bromoquinoline *N*-oxide (**2**) (1.27 g, 5.7 mmol) and sodium hydroxide (0.44 g, 11.0 mmol) in water (12.0 mL) and CH_2Cl_2 (6.0 mL), benzoyl chloride (8.5 mmol, 1.0 mL) was added slowly to the vigorously stirred mixture [15]. A reflux was observed when the addition was nearly completed. Then the flask was then cooled to 5 °C with ice-bath, and addition was resumed. After 1 h

stirring, the precipitate was filtered off, rinsed well with water (50 mL) and CH_2Cl_2 (50 mL) respectively, then dried in the air, white product was obtained.

To a re-sealable Schlenk tube was charged the white product, POBr_3 (2.20 g, 7.7 mmol, 1.5-2 equiv.) and dry toluene (5.0 mL) as the solvent under N_2 , heated to reflux overnight. After cooling to r.t., the mixture was poured on ice, washed with saturated NaHCO_3 and extracted with CH_2Cl_2 several times. Remove the solvent under reduced pressure. Off-white solid was afforded (1.16 g, 70.5% yield), m.p. 160-163 °C. ^1H NMR (400 MHz, CDCl_3) δ (ppm): 7.99 (d, $J = 2.1$ Hz, 1H), 7.94 (t, $J = 8.6$ Hz, 2H), 7.82 (dd, $J_1 = 9.0$ Hz, $J_2 = 2.1$ Hz, 1H), 7.56 (d, $J = 8.6$ Hz, 1H).

2.4.4. Synthesis of 6-bromoquinolin-2-amine (**4**)

To a round bottom flask was charged **2** (2.24 g, 10.0 mmol, 1.0 equiv), 40 mL trifluorotoluene and 20 mL chloroform under N_2 . After compound **2** was dissolved, the mixture was cooled to 0-10 °C with an ice-bath. *t*-butylamine (5.3 mL, 50.0 mmol, 5.0 equiv) was added followed by Ts_2O (6.50 g, 20.0 mmol, 2.0 equiv) while the temperature was kept at 5-12 °C. If the reaction was not completed within 30 min, portions of *t*-butylamine (0.6 equiv. to 4.0 equiv.) and Ts_2O (0.3 equiv. to 2.3 equiv.) would be charged until the reaction completed. The reaction was then treated with TFA 25 mL at 70 °C for 10 h. Most of the solvents could be removed under vacuum. The oil residue was diluted with CH_2Cl_2 and quenched with 50% aq solution NaOH to pH 9-10. The aqueous layer was extracted with CH_2Cl_2 (50 mL) three times. The combined organic layers were dried with MgSO_4 . The solvent was removed by reduced pressure

and the crude product was then purified by silica gel column chromatography (2% MeOH/CH₂Cl₂) to give the desired **4** as a gray solid (1.75 g, 78.3% yield), m.p. 139-145 °C (lit. [16] 141-146 °C). ¹H NMR (400 MHz, CDCl₃) δ (ppm): 7.79 (d, *J* = 8.8 Hz, 1H), 7.76 (d, *J* = 2.2 Hz, 1H), 7.61 (dd, *J*₁ = 8.9 Hz, *J*₂ = 2.2 Hz, 1H), 7.52 (d, *J* = 8.9 Hz, 1H), 6.73 (d, *J* = 8.8 Hz, 1H), 4.83 (s, 2H).

2.4.5. Synthesis of bis(6-bromoquinolin-2-yl)amine (**5**)

To a re-sealable Schlenk tube was charged with bis(2-diphenylphosphinophenyl) ether (0.3016 g, 0.560 mmol, 4% mmol), **4** (3.28 g, 14.7 mmol), 2,6-dibromoquinoline **3** (4.00 g, 14.0 mmol), *t*-BuONa (1.88 g, 19.6 mmol), and degassed dry toluene (120 mL). The Schlenk tube was capped and carefully subjected to three cycles of evacuation-backfilling with N₂. Finally, Pd(OAc)₂ (0.1258 g, 0.560 mmol, 4% mmol) was added. It was then sealed and immersed into a 110 °C oil bath. After 5 h reflux, the mixture was cooled to r.t., diluted with THF and ethyl ether, filtered, concentrated, and purified by silica gel column chromatography (2% MeOH/CH₂Cl₂) to afford the product. White solid (5.30 g, 88.2% yield), m.p. 237-238 °C. ¹H NMR (400 MHz, DMSO-*d*₆) δ (ppm): 10.63 (s, 1H), 8.26 (s, 4H), 8.13 (d, *J* = 2.0 Hz, 2H), 7.81 – 7.72 (m, 4H). ¹³C NMR (101 MHz, CDCl₃) δ (ppm): 152.63, 145.85, 137.08, 133.19, 129.56, 128.81, 126.08, 117.55, 114.84. TOF-MS (ES⁺) calcd. for C₁₈H₁₁Br₂N₃ [M + 1]⁺: 427.9, found 428.1. Elemental analysis calcd. (%) for C₁₈H₁₁Br₂N₃: C, 50.38; H, 2.58; N, 9.79, found C, 50.08; H, 2.53; N, 10.15.

2.4.6. Synthesis of bis(6-phenylquinolin-2-yl)amine (**8a**)

To a round bottom flask was charged **5** (1.00 g, 2.3 mmol), K_2CO_3 (0.63 g, 4.6 mmol), $Pd(dppf)_2Cl_2$ (0.0673 g, 0.0920 mmol, 0.4% mol), benzenboronic acid **6a** (0.85 g, 7.0 mmol) [17]. The flask was capped and carefully subjected to three cycles of evacuation-backfilling with N_2 . A degassed solution of dioxane/ H_2O (3:1 v/v) 10 mL was then injected to the system and heated to reflux with oil bath for 12 h. After cooling to r.t., it was diluted with CH_2Cl_2 (100 mL) and filtered. The filtration was then dried with Na_2SO_4 and the solvent was removed under reduced pressure. The crude product was purified by silica gel column chromatography (2% MeOH/ CH_2Cl_2). White solid was afforded (0.91 g, 93.2% yield), m.p. 249-255 °C. 1H NMR (400 MHz, DMSO- d_6) δ (ppm): 10.58 (s, 1H), 8.33 (dd, $J_1 = 22.7$ Hz, $J_2 = 9.0$ Hz, 4H), 8.18 (d, $J = 2.1$ Hz, 2H), 8.02 (dd, $J_1 = 8.7$ Hz, $J_2 = 2.1$ Hz, 2H), 7.89 (d, $J = 8.7$ Hz, 2H), 7.82 (d, $J = 7.2$ Hz, 4H), 7.53 (t, $J = 7.7$ Hz, 4H), 7.40 (t, $J = 7.4$ Hz, 2H). ^{13}C NMR (101 MHz, DMSO- d_6) δ (ppm): 153.32, 146.12, 137.92, 135.19, 129.02, 128.64, 127.35, 127.04, 126.71, 125.12, 124.71, 114.82. TOF-MS (ES^+) calcd. for $C_{30}H_{21}N_3$ [$M + 1$] $^+$: 424.2, found 424.2. Elemental analysis calcd. (%) for $C_{30}H_{21}N_3$: C, 85.08; H, 5.00; N, 9.92, found C, 85.34; H, 4.79; N, 9.87.

2.4.7. Synthesis of bis(6-(4-(tert-butyl)phenyl)quinolin-2-yl)amine (**8b**)

Compound **8b** was synthesized according to the method described for compound **8a**. Yellow solid was afforded, the yield was 90.5%, m.p. > 300 °C. 1H NMR (400 MHz, $CDCl_3$) δ (ppm): 8.16 (d, $J = 8.9$ Hz, 1H), 8.05 (d, $J = 8.9$ Hz, 1H), 7.93 (s, 3H), 7.67 (d,

$J = 8.3$ Hz, 2H), 7.52 (d, $J = 8.4$ Hz, 2H), 1.39 (s, 9H). TOF-MS (ES^+) calcd. for $\text{C}_{38}\text{H}_{37}\text{N}_3$ [$\text{M} - t\text{-BuPh} + 1$] $^+$: 404.2, found 404.2. Elemental analysis calcd. (%) for $\text{C}_{38}\text{H}_{37}\text{N}_3$: C, 85.19; H, 6.96; N, 7.84, found C, 85.23; H, 7.00; N, 7.77.

2.4.8. Synthesis of bis(6-(4-(diphenylamino)phenyl)quinolin-2-yl)amine (**8c**)

Compound **8c** was synthesized according to the method described for compound **8a**. Red solid was afforded, the yield was 88.7%, m.p. 278-279 °C. ^1H NMR (400 MHz, $\text{DMSO-}d_6$) δ (ppm): 10.52 (s, 1H), 8.35 – 8.21 (m, 4H), 8.10 (d, $J = 1.9$ Hz, 2H), 7.96 (dd, $J_1 = 8.8$ Hz, $J_2 = 2.0$ Hz, 2H), 7.83 (d, $J = 8.8$ Hz, 2H), 7.73 (d, $J = 8.7$ Hz, 4H), 7.38 – 7.27 (m, 8H), 7.05-7.09 (m, 16H). ^{13}C NMR (101 MHz, CDCl_3) δ (ppm): 152.56, 147.66, 147.29, 146.23, 138.18, 136.28, 134.42, 129.33, 129.12, 127.84, 127.29, 125.23, 124.61, 124.48, 123.99, 123.02, 114.46. TOF-MS (ES^+) calcd for $\text{C}_{54}\text{H}_{39}\text{N}_5$ [$\text{M} - \text{C}_{27}\text{H}_{19}\text{N}_2 + 1$] $^+$: 387.2, found 387.1. Elemental analysis calcd. (%) for $\text{C}_{54}\text{H}_{39}\text{N}_5$: C, 85.57; H, 5.19; N, 9.24, found C, 85.32; H, 5.14; N, 9.39.

2.4.9. Synthesis of difluoro-boron complex of bis(6-bromoquinolin-2-yl)amine (**7**)

To a three-necked round bottom flask was charged **5** (1.40 g, 3.3 mmol) and dry toluene under N_2 . DIEA (1.6 mL, 9.9 mmol) was slowly injected to the toluene solution. After 10 minutes' stirring, $\text{BF}_3 \cdot \text{Et}_2\text{O}$ (3.5 mL, 13.2 mmol) was injected dropwise to the solution. The reaction was then refluxed overnight. After cooling to room temperature, the precipitate was filtered off and dried in air for 2 h. The precipitate was added into 100 mL water and stirred for 30 min, adjusted pH to 7 with saturated NaHCO_3 . Filtrated

and dried in the air for 2 h, washed with diethyl ether and isopropyl ether respectively to give the crude product. It was then purified by silica column chromatography (CH_2Cl_2) to afford **7** as a yellow solid (1.27 g, 80.6% yield), m.p. > 300 °C. ^1H NMR (400 MHz, $\text{DMSO}-d_6$) δ (ppm): 8.40 – 8.31 (m, 2H), 8.29 (d, $J = 2.3$ Hz, 1H), 8.00 (dd, $J_1 = 9.3$ Hz, $J_2 = 2.4$ Hz, 1H), 7.35 (d, $J = 9.1$ Hz, 1H). ^{19}F NMR (376 MHz, $\text{DMSO}-d_6$) δ (ppm): -125.14 (q, $J_{\text{B,F}} = 75.2$ Hz). TOF-MS (ES^+) calcd for $\text{C}_{18}\text{H}_{10}\text{BBr}_2\text{F}_2\text{N}_3$ [$\text{M} - \text{Br}_2 + 1$] $^+$: 318.09, found 318.3. Elemental analysis calcd. (%) for $\text{C}_{18}\text{H}_{10}\text{BBr}_2\text{F}_2\text{N}_3$: C, 45.33; H, 2.11; N, 8.81, found C, 45.36; H, 2.35; N, 8.50.

2.4.10. Synthesis of difluoro-boron complex of bis(6-phenylquinolin-2-yl)amine (**B1**)

Complex **B1** can be synthesized from both of the two synthetic routes, one described for **8a** via a boron complexation with complex **7** and the other described for **7** via a Suzuki coupling with **8a**, as shown in Scheme 2. In comparison, route 2 shows a higher overall yield (80.1%) with more synthetic steps, while route 1 exhibits a more straightforward way to obtain the target products. **B1** was obtained as bright yellow solid, the yield was 75.6% (route 1) and 80.1% (route 2), m.p. 269-270 °C. ^1H NMR (400 MHz, CDCl_3) δ (ppm): 8.72 (d, $J = 9.1$ Hz, 1H), 8.08 (d, $J = 9.1$ Hz, 1H), 7.99 (dd, $J_1 = 9.1$ Hz, $J_2 = 2.1$ Hz, 1H), 7.89 (d, $J = 2.0$ Hz, 1H), 7.70 (d, $J = 7.3$ Hz, 2H), 7.51 (t, $J = 7.6$ Hz, 2H), 7.41 (t, $J = 7.3$ Hz, 1H), 7.24 (d, $J = 9.1$ Hz, 1H). ^{13}C NMR (101 MHz, CDCl_3) δ (ppm): 154.09, 140.73, 139.54, 137.94, 137.70, 130.37, 129.04, 127.83, 127.17, 126.04, 125.07, 123.11, 122.26. ^{19}F NMR (376 MHz, CDCl_3) δ (ppm): -126.54 (q, $J_{\text{B,F}} = 75.2$ Hz). TOF-MS (ES^+) calcd. for $\text{C}_{30}\text{H}_{20}\text{BF}_2\text{N}_3$ [$\text{M} + 1$] $^+$: 472.2, found

472.1. Elemental analysis calcd. (%) for $C_{30}H_{20}BF_2N_3$: C, 76.45; H, 4.28; N, 8.92, found C, 76.37; H, 4.42; N, 8.90.

2.4.11. *Synthesis of difluoro-boron complex of bis(6-(4-(tert-butyl)phenyl)quinolin-2-yl)amine (B2)*

Complex **B2** was synthesized according to the method described for complex **B1**. Bright yellow solid, the yield was 72.3% (route 1) and 83.1% (route 2) respectively, m.p. > 300 °C. 1H NMR (400 MHz, $CDCl_3$) δ (ppm): 8.70 (d, $J = 9.0$ Hz, 1H), 8.05 (d, $J = 9.1$ Hz, 1H), 7.99 (dd, $J_1 = 9.1$ Hz, $J_2 = 2.1$ Hz, 1H), 7.87 (d, $J = 2.0$ Hz, 1H), 7.64 (d, $J = 8.3$ Hz, 2H), 7.53 (d, $J = 8.4$ Hz, 2H), 7.21 (d, $J = 9.0$ Hz, 1H), 1.39 (s, 9H). ^{19}F NMR (376 MHz, $CDCl_3$) δ (ppm): -126.59 (q, $J_{B,F} = 71.4$ Hz). HR-MS-ESI⁺ calcd. for $C_{38}H_{36}BF_2N_3$ [M + 1]⁺: 584.2970, found 584.3054. Elemental analysis calcd. (%) for $C_{38}H_{36}BF_2N_3$: C, 78.22; H, 6.22; N, 7.20, found C, 78.13; H, 6.31; N, 7.15.

2.4.12 *Synthesis of difluoro-boron complex of bis(6-(4-(trifluoromethyl)phenyl)quinolin-2-yl)amine (B3)*

Complex **B3** was synthesized according to the method described for compound **8a** using **7** and **6c** as reactants. Bright yellow solid, the yield was 85.6%, m.p. > 300 °C. 1H NMR (400 MHz, $CDCl_3$) δ (ppm): 8.75 (d, $J = 9.2$ Hz, 1H), 8.11 (d, $J = 9.0$ Hz, 1H), 7.99 (dd, $J_1 = 9.0$ Hz, $J_2 = 2.1$ Hz, 1H), 7.93 (d, $J = 1.9$ Hz, 1H), 7.79 (dd, $J_1 = 18.5$ Hz, $J_2 = 8.3$ Hz, 4H), 7.29 (s, 1H). ^{19}F NMR (376 MHz, $CDCl_3$) δ (ppm): -126.35 (q, $J_{B,F} = 71.4$ Hz). HR-MS-ESI⁺ calcd. for $C_{32}H_{18}BF_8N_3$ [M + 1]⁺: 608.1466, found 608.1546.

Elemental analysis calcd. (%) for $C_{32}H_{18}BF_8N_3$: C, 63.29; H, 2.99; N, 6.92, found C, 63.38; H, 3.21; N, 6.64.

2.4.13 Synthesis of difluoro-boron complex of bis(6-(4-nitro)phenyl)quinolin-2-yl)amine (**B4**)

Complex **B4** was synthesized according to the method described for compound **8a** using **7** and **6d** as reactants. Bright yellow solid, the yield was 67.6%, m.p. > 300 °C. This complex exhibits poor solubility in many solvents, which makes it hard to get 1H NMR. Elemental analysis calcd. (%) for $C_{30}H_{18}BF_2N_5O_4$: C, 64.19; H, 3.23; N, 12.48, found C, 64.78; H, 3.07; N, 12.66.

2.4.14 Synthesis of difluoro-boron complex of bis(6-(4-(9H-carbazol-9-yl)phenyl)quinolin-2-yl)amine (**B5**)

Complex **B5** was synthesized according to the method described for compound **8a** using **7** and **6e** as reactants. Bright yellow solid, the yield was 78.1%, m.p. > 300 °C. 1H NMR (400 MHz, DMSO- d_6) δ (ppm): 8.63 (d, $J = 9.2$ Hz, 1H), 8.52 (d, $J = 9.1$ Hz, 1H), 8.49 (d, $J = 2.1$ Hz, 1H), 8.36 (dd, $J_1 = 9.2$ Hz, $J_2 = 2.2$ Hz, 1H), 8.30 (d, $J = 7.8$ Hz, 2H), 8.18 (d, $J = 8.5$ Hz, 2H), 7.84 (d, $J = 8.5$ Hz, 2H), 7.56 – 7.45 (m, 4H), 7.40 (d, $J = 9.1$ Hz, 1H), 7.36 – 7.29 (m, 2H). ^{19}F NMR (376 MHz, DMSO- d_6) δ (ppm): -125.04 (q, $J_{B,F} = 75.2$ Hz). Elemental analysis calcd. (%) for $C_{54}H_{34}BF_2N_5$: C, 80.90; H, 4.27; N, 8.74, found C, 80.79; H, 4.35; N, 8.77.

2.4.15 Synthesis of difluoro-boron complex of bis(6-(4-(diphenylamino)phenyl)quinolin-2-yl)amine (**B6**)

Complex **B6** was synthesized according to the method described for complex **B1**. Orange solid, the yield was 73.8% (route 1), 78.0% (route 2), m.p. 264-267 °C. ^1H NMR (400 MHz, DMSO- d_6) δ (ppm): 8.64 (d, $J = 9.1$ Hz, 1H), 8.56 (d, $J = 8.8$ Hz, 1H), 8.39 (d, $J = 1.9$ Hz, 1H), 8.28 (dd, $J_1 = 9.3$ Hz, $J_2 = 1.9$ Hz, 1H), 7.80 (d, $J = 8.7$ Hz, 2H), 7.48 (d, $J = 9.1$ Hz, 1H), 7.36 (t, $J = 7.9$ Hz 4H), 7.09 – 7.13 (m, 8H). ^{19}F NMR (376 MHz, DMSO- d_6) δ (ppm): -125.12 (q, $J_{\text{B,F}} = 82.7$ Hz). Elemental analysis calcd. (%) for $\text{C}_{54}\text{H}_{38}\text{BF}_2\text{N}_5$: C, 80.50; H, 4.75; N, 8.69, found C, 80.60; H, 4.35; N, 8.86.

3. Results and discussion

3.1. Synthesis and characterization

Scheme 2 outlines the synthetic route for complexes **B1-B6**. The boronic acids (**6a-6f**) were synthesized according to the literature procedures [9]. Both intermediates **3** and **4** were prepared from compound **2** respectively, in which compound **4** was obtained via a two-step-synthesis involving a procedure of *t*-butyl protection and deprotection. In addition, when the mixture of trifluorotoluene/ CHCl_3 (2:1 v/v) was used as solvent instead of trifluorotoluene in the synthetic procedure of **4**, the yield increased from 47.3% to 73.5%. The intermediate bis(6-bromoquinolin-2-yl)amine (**5**) was tried to synthesized by using quinoline *N*-oxide as starting material, then tosylation by 4-toluene sulfonyl chloride (TsCl) and amination by ammonia gas to afford the desired product. This is supposed to be the simplest method to obtain diquinolinamine

derivatives, which was reported by Couturier and co-workers [18] in 2006 (Scheme S1). However, no target product but 2-hydroxyquinoline was afforded in 73.6% yield in this work. Although other quinoline *N*-oxides derivatives were attempted as starting materials, 2-hydroxyquinoline derivatives were obtained. Finally, as shown in Scheme 2, compound **5** was synthesized by **3** and **4** in the presence of Pd-catalyst and *t*-BuONa in 88.2% yield.

As shown in Scheme 2, two different synthetic routes (route 1 and route 2) could be utilized to prepare the target complexes (**B1–B6**), depending on the designed substituents on the aza-BODIQU moiety and the reaction sequence of Suzuki coupling and boron complexation. In comparison, route 2 exhibits a higher overall yield for **B1**, **B2** and **B6** than route 1. However, in terms of versatile synthesis of the target complexes, route 1 takes less intermediates, which is approved a better synthetic route for all complexes. In addition, the final complexation step was achieved via modified procedure reported by Bañuelos and co-workers [6]. The crude product was purified by washing with water, diethyl ether and isopropyl ether, respectively. All complexes (**B1–B6**) are air-stable and soluble in CH₂Cl₂, CHCl₃, acetone, tetrahydrofuran, DMF and dimethyl sulfoxide. ¹H NMR, ¹⁹F NMR and elemental analyses confirmed the proposed structures for all complexes except **B4**, due to its poor solubility. ¹³C NMR data was not obtained due to the poor solubility of this sample, although different solvents were attempted.

3.2. Thermal properties

The thermal properties of aza-boron-diquinomethene **B1-B6** were investigated by differential scanning calorimetry (DSC) analyses, shown in Table 1. Complexes **B1-B6** are thermally stable and lack any detectable phase transitions from 50 °C to 230 °C (Fig. S7). Compared with other complexes in this series, the T_g and T_m of **B2** and **B4** were not observed in the scan scale from 50 °C to 400 °C, which indicating their robust thermal stability at this temperature range. Furthermore, complex **B2** exhibits interesting exothermic peak which may result from the crystallizing progress while others exhibit endothermic peaks. All these complexes exhibit good thermal stability with high glass transition temperatures (> 187 °C) and melt transitions temperatures (> 257 °C), which is required for the thermal stability of the OLED devices.

3.3. Electronic absorption

The UV-Vis absorption of **B1-B6** obeys Lambert-Beer's law in the concentration range studied (2×10^{-5} - 2×10^{-7} mol L⁻¹) in CH₂Cl₂, suggesting that no dimerization or oligomerization occurs within this concentration range in CH₂Cl₂. The UV-Vis absorption and emission spectra of **B1-B6** in CH₂Cl₂ and in the solid state are shown in Fig. 1 and Fig. 2, respectively. The photophysical parameters are summarized in Table 2. As shown in Fig. 1 and Table 2, complexes **B1-B5** show sharp and strong absorption ($\epsilon = 5.6 \times 10^4$ to 8.2×10^4 L mol⁻¹ cm⁻¹) in the range of 401 nm to 457 nm in CH₂Cl₂ solution, while complex **B6** shows a relatively broad band ($\epsilon = 2.5 \times 10^4$ L mol⁻¹ cm⁻¹)

at 471 nm. The absorption bands of **B1-B5** can be assigned to the $^1\pi-\pi^*$ transition localized on the conjugated aromatic rings, considering their intense and structured absorption bands and minor solvatochromic effect (Fig. S2). The bathochromically shift in complex **B6** could be attributed to a $^1\pi-\pi^*$ mixed intramolecular charge transfer (^1ICT) transition, which is originated from the appended strong electron-donating NPh_2 substituents to the central aza-BODIQU component. Compared to the ground-state absorption of difluoro-boron-triaza-anthracene (BTAA) [6] (*i.e.* the parent complex), complexes **B1-B6** with different substituents exhibit a significant increase of the absorption coefficients and the $^1\pi-\pi^*$ transition bands bathochromically shift. The minor solvent effect (in Supporting information, Fig. S2) also supports the $^1\pi-\pi^*$ assignment for their absorption bands. In addition, compared with the absorption spectra in solution, broader absorption bands with significant bathochromic shifts are observed in the solid state (Fig. 2 and Table 2). This could be attributed to the molecular stacking in the solid state, which suggests an increased conjugation length in their solid state due to the π -stacking of the planar conformations of aza-boron-diquinomethene. The assignment of the absorption band is also supported by the density functional theory (DFT) and time-dependent density function theory (TDDFT) calculations, which will be discussed in the following section.

3.4. Theoretical calculations

The ground-state electron density distribution of the HOMO (highest occupied molecular orbital) and LUMO (lowest unoccupied molecular orbital) are illustrated in

Fig. 3. The HOMO-LUMO energy differences (energy band gaps, calculated E_g^{cal}) are presented in Table 3. Due to the nearly coplanar geometry, the π -electrons in the HOMO of **B1-B6** are delocalized over the entire molecule backbone, offering effective orbital interactions among the stacked π -systems, while their LUMOs are mainly localized on the aza-BODIQU moieties. Therefore, the HOMO→LUMO transition that is the dominant contributing configuration to the S_1 state in **B1-B6** should be ascribed to a mixture of $^1\pi\text{-}\pi^*$ and ICT characters, which is consistent with their UV-Vis absorption assignments. The results clearly demonstrate that strong electron-donating substituent, such as NPh_2 in **B6**, increases the energy level of HOMO more than that of LUMO, thus the HOMO-LUMO gap decreases, causing a red-shift of the $^1\pi\text{-}\pi^*/\text{ICT}$ band. This trend follows that observed from the UV-Vis absorption measurement. Compared to **B1**, when electron-withdrawing substituents such as CF_3 and NO_2 groups are introduced on the phenyl ring in **B3** and **B4**, their HOMOs and LUMOs are almost delocalized on the whole molecule. Meanwhile, when the *t*-Bu, carbazolyl and NPh_2 are chosen as electron-donating substituents in **B2**, **B5** and **B6**, their LUMOs are mainly delocalized on the aza-BODIQU components. However, in the case of **B5** and **B6**, calculations indicate that ICT transition occurred from the carbazolyl and NPh_2 groups to their aza-BODIQU moieties. This could also explain the bathochromic shifts observed in the absorption of **B5** and **B6** compared with other complexes, especially for **B6** bearing strong electron-donating substituents like NPh_2 [19]. As is evident from Table 3, the trend of the predicted E_g^{cal} values (3.17-3.70 eV) is in consistent with the estimated E_g^{opt} (energy band gaps, calculated from the ground-state absorption,

2.45-2.70 eV) in Table 2.

3.5. Photoluminescence

The photoluminescence of complexes **B1-B6** in different solvents were investigated at room temperature. Their normalized emission spectra in CH_2Cl_2 at a concentration of 1×10^{-7} mol/L are illustrated in Fig. 1. The emission band maxima and quantum yields are listed in Table 2. Excitations of these compounds at their respective absorption band maximum at room temperature results in structured blue to green luminescence, as shown in Fig. 1. The Stokes shifts of these compounds are quite small and the emission lifetimes are in the nanosecond regime (Table 2). Taking these features into account, we can assign the observed emission to the $^1\pi\text{-}\pi^*$ state. Furthermore, tailed spectra are observed in the region of 500-550 nm. This indicates that their emission colors contain more blue but less greenish component, which is desirable for the blue or blue-green light emitting materials. It is noted that the emission of **B6** is quite different from that of other complexes, due to the ICT process [20] caused by the NPh_2 substituent with strong electron-donating ability. The significant bathochromic shift of **B6** in both absorption and emission spectra are observed, owing to the intra-molecular electron push-pull effect.

The photoluminescence quantum yields (Φ_{PL}) of the **B1-B6** were measured in CH_2Cl_2 solution, using compound 9,10-diphenylanthracene as standard ($\Phi_{\text{PL}} = 0.97$ in cyclohexane solution) at r.t. [21]. All the complexes exhibit relatively high Φ_{PL} in the range of 0.47-0.93, except for complex **B6** ($\Phi_{\text{PL}} = 0.01$). Their Φ_{PL} in CH_2Cl_2 solution

follow the trend of **B1** > **B2** > **B5** > **B3** > **B4** > **B6**, in which complex **B1** exhibits the highest photoluminescence quantum yield ($\Phi_{\text{PL}} = 0.93$). When the core structure was substituted with either electron-withdrawing or electron-donating groups, the Φ_{PL} of the complexes decreased. Additionally, the complexes with electron-withdrawing substituents exhibit relative lower photoluminescence quantum yields compared to those with electron-donating substituents. The emission quenching of **B6** is induced by the ICT process, due to the strong electron-donating effect of NPh_2 substituent [20].

Solvent dependence study was performed in solvents with various polarities, such as hexane, toluene, CH_2Cl_2 , THF, acetonitrile and methanol (Fig. S2-3). The minor solvatochromic effect and structured emission bands observed for **B1-B5** indicate the $^1\pi\text{-}\pi^*$ dominated features of their emitting states. However, the emission bands of complex **B6** bathochromically shift to longer wavelengths in more polar solvents (*i.e.*, CH_2Cl_2 and THF) compared to those in solvents with lower polarity (*i.e.*, hexane and toluene), as exemplified in Fig. 4. The drastic positive solvatochromic effect observed in **B6** but not in the other complexes should be attributed to the electron-donating groups (NPh_2), which enhances electron transfer from the symmetrical peripheral chromophores to the aza-BODIQU motif. This feature is commonly seen from compounds with charge transfer character, and also supported by the DFT calculation results.

3.6. Electrochemical Properties.

The electrochemical properties of complex **B1-B6** were determined by cyclic

voltammetry (CV) in a mixed solvent of CH₃CN/CH₂Cl₂ (7:3 v/v) at a scan rate of 100 mV s⁻¹ using tetra-*n*-butylammonium perchlorate as supporting electrolyte. Potentials were standardized with ferrocene-ferrocenium (Fc/Fc⁺) couple as internal reference vs Ag/AgNO₃. The cyclic voltammograms of **B1-B6** are illustrated in Fig. 5, and their electrochemical properties are summarized in Table 4. As shown in Fig. 5, cyclic voltammograms of **B1-B6** all exhibit oxidation waves (0.58-1.07 V). However, the electroreduction processes are observed only in **B1, B3, B4**, while reduction process do not exist in electron-withdrawing substituted complexes (**B2, B5, B6**), it is thought that the electronic factors on the aza-BODIQU moiety may be the main possible reason for the less sensitivity of the reduction potentials [22]. Corresponding energy levels of the HOMOs for **B1-B6** are calculated from the onset of the oxidation peaks. Cyclic voltammogram of **B1** shows three electro-oxidation processes (0.70-1.63 V). Among them, only **B6** shows one reversible cathodic wave with a monoelectronic exchange, which can be attributed to the oxidation of NPh₂ substituents of aza-BODIQU to its radical cation (**B6/B6⁺**) [23]. As presented in Table 3, the calculated HOMO levels are ranging from -5.28 ~ -5.61 eV and the LUMO energy levels were estimated in the range of -2.63 ~ -2.95 eV, which are close to the LUMO level of AlQ₃ (a widely used electron transporting chelate and a green emitter, LUMO = 2.8 eV) [24]. These results suggest that these complexes are potential electron-transporting (*n*-type) materials for OLEDs.

4. Conclusions

In summary, we present the synthesis of aza-boron-diquinomethene complexes (**B1-B6**) and the symmetrical synthesis for aza-diquinomethene and its derivatives with high efficiency and selectivity. Electron-donor and electron-acceptor were introduced to the system and their thermal stabilities, photophysical properties, electrochemical behaviors and theoretical calculations were investigated systematically. These materials showed robust thermal stability with high glass transition temperatures ($> 187\text{ }^{\circ}\text{C}$) and melt transitions temperatures ($> 257\text{ }^{\circ}\text{C}$). Absorption and emission spectra were recorded in both CH_2Cl_2 solution and solid states. All complexes exhibit strong ${}^1\pi\text{-}\pi^*$ absorption in the visible spectral region, while strong electron-donating substituent NPh_2 causes a red-shift of the ${}^1\text{ICT}/{}^1\pi\text{-}\pi^*$ band. The assignment of the absorption bands is supported by DFT calculations. All complexes exhibit intense blue to green ${}^1\pi\text{-}\pi^*/{}^1\text{ICT}$ emission with relative high photoluminescence quantum yields (0.47-0.93), except for **B6** ($\Phi_{\text{PL}} = 0.01$). Their photoluminescence quantum yields follow the trend of **B1** $>$ **B2** $>$ **B5** $>$ **B3** $>$ **B4** $>$ **B6**. Moreover, these complexes show the low-lying LUMO energy levels ($-2.63 \sim -2.92\text{eV}$), which is desirable for electron transfer. The robust thermal stability, intense blue emission and relatively high photoluminescence quantum yields suggest that these complexes could be promising candidates as organic light-emitting materials.

Acknowledgment.

We greatly acknowledge the financial support in part by Postgraduate Innovation Fund of Jiangsu Province (2011, CXZZ11_0366) and Innovation program of Shanghai

institute of technical physics of the Chinese academy of sciences (2013, Q-DX-36, Q-DX-37).

Supporting information

Synthetic route of diquinolinamines. Emission spectra of **B1-B6** in the solid state and in CH_2Cl_2 solution. Normalized absorption and emission spectra of **B1-B6** in different solvents. Absorption and emission spectra of **B1-B6** in CH_2Cl_2 of different concentrations. DSC thermograms of **B1-B6**. Detailed DFT and TDDFT calculation results for **B1-B6**.

References:

- [1] (a) Loudet A, Burgess K. BODIPY dyes and their derivatives: syntheses and spectroscopic properties. *Chem Rev* 2007;107:4891-932; (b) Boens N, Leen V, Dehaen W. Fluorescent indicators based on BODIPY. *Chem Soc Rev* 2012;41:1130-72; (c) Kamkaew A, Lim SH, Lee HB, Kiew LV, Chung LY, Burgess K. BODIPY dyes in photodynamic therapy. *Chem Soc Rev* 2013;42:77-88; (d) Zhang ZY, Xu B, Su JH, Shen LP, Xie YS, Tian H. Color-tunable solid-state emission of 2,2'-biindenyl-based fluorophores. *Angew Chem Int Ed* 2011;50:11654-7. (e) Zhou Y, Xiao Y, Chi SM, Qian XH. Isomeric boron-fluorine complexes with donor-acceptor architecture: strong solid/liquid fluorescence and large stokes shift. *Org Lett* 2008;10:633-6; (f) Ulrich G, Ziessel R, Harriman A. The chemistry of fluorescent BODIPY dyes: versatility unsurpassed. *Angew Chem Int Ed* 2008;47:1184-201; (g) Ziessel R, Ulrich G, Harriman A. The chemistry of BODIPY: a new El Dorado for fluorescence tools. *New J Chem* 2007;31:496-501; (h) Zhou Y, Xiao Y, Li D, Fu MY, Qian XH. Novel fluorescent fluorine-boron complexes: synthesis, crystal structure, photoluminescence, and electrochemistry properties. *J Org Chem* 2008;73:1571-4.
- [2] (a) Poirel A, Nicola AD, Ziessel R. Oligothieryl-BODIPYs: red and near-infrared emitters. *Org Lett* 2012;14:5696-9; (b) Gao L, Deligonul N, Gray TG. Gold(I) complexes of brominated azadipyromethene ligands. *Inorg Chem* 2012;51:7682-8; (c) Kubota Y, Tsuzuki T, Funabiki K, Ebihara M, Matsui M. Synthesis and fluorescence properties of a pyridomethene-BF₂ complex. *Org Lett* 2010;12:4010-3; (d) Li HJ, Fu WF, Li L, Gan X, Mu WH, Chen WQ, et al. Intense one- and two-photon excited

fluorescent bis(BF₂) core complex containing a 1,8-naphthyridine derivative. *Org Lett* 2010;12:2924-7; (e) Murtagh J, Frimannsson DO, O'Shea DF. Azide conjugatable and pH responsive near-infrared fluorescent imaging probes. *Org Lett* 2009;11:5386-9; (f) Adarsh N, Avirah RR, Ramaiah D. Tuning photosensitized singlet oxygen generation efficiency of novel aza-BODIPY dyes. *Org Lett* 2010;12:5720-3; (g) Chibani S, Guennic BL, Charaf-Eddin B, Maury O, Andraud C, Jacquemin D. On the computation of adiabatic energies in aza-boron-dipyrrromethene dyes. *J Chem Theory Comput* 2012;8:3303-13.

[3] (a) Sasabe H, Kido J. Multifunctional materials in high-performance OLEDs: challenges for solid-state lighting. *Chem Mater* 2011;23:621-30; (b) Hayashi Y, Obata N, Tamaru M, Yamaguchi S, Matsuo Y, Saeki A, et al. Facile synthesis of biphenyl-fused BODIPY and its property. *Org Lett* 2012;14:866-9; (c) Li Y, Dolphin D, Patrick BO. Synthesis of a BF₂ complex of indol-2-yl-isoindol-1-ylidene-amine: a fully conjugated azadipyrrromethene. *Tetrahedron Lett* 2010;51:811-4; (d) Forgie JC, Skabara PJ, Stibor I, Vilela F, Vobecka Z. New redox stable low band gap conjugated polymer based on an EDOT-BODIPY-EDOT repeat unit. *Chem Mater* 2009;21:1784-6; (e) Hepp A, Uirich G, Schmechel R, von Seggern H, Ziessel R. Highly efficient energy transfer to a novel organic dye in OLED devices. *Synth Met* 2004;146:11-15.

[4] (a) Wen SW, Lee MT, Chen CH. Recent development of blue fluorescent OLED materials and devices. *J Disp Technol* 2005;1:90-9; (b) Huang JH, Su JH, Tian H. The development of anthracene derivatives for organic light-emitting diodes. *J Mater Chem* 2012;22:10977-89; (c) Yeh SJ, Wu MF, Chen CT, Song YH, Chi Y, Ho MH et al. New

dopant and host materials for blue-light-emitting phosphorescent organic electroluminescent devices. *Adv Mater* 2005;17:285-9.

[5] Sathyamoorthi G, Soong ML, Ross TW, Boyer JH. Fluorescent tricyclic β -azavinamidine-BF₂ complexes. *Heteroat Chem* 1993;4:603-8.

[6] Bañuelos J, Arbeloa FL, Martinez V, Liras M, Costela A, Moreno IG, et al. Difluoro-boron-triaza-anthracene: a laser dye in the blue region. Theoretical simulation of alternative difluoro-boron-diaza-aromatic systems. *Phys Chem Chem Phys* 2011;13:3437-45.

[7] (a) Ahmed E, Earmme T, Jenekhe SA. New solution-processable electron transport materials for highly efficient blue phosphorescent OLEDs. *Adv Funct Mater* 2011;21:3889-99; (b) Tonzola CJ, Kulkarni AP, Gifford AP, Kaminsky W, Jenekhe SA. Blue-light-emitting oligoquinolines: synthesis, properties, and high-efficiency blue-light-emitting diodes. *Adv Funct Mater* 2007;17:863-74; (c) Tonzola CJ, Alam MM, Bean BA, Jenekhe SA. New soluble *n*-type conjugated polymers for use as electron transport materials in light-emitting diodes. *Macromolecules* 2004;37:3554-63; (d) Tonzola CJ, Alam MM, Bean BA, Jenekhe SA. A new synthetic route to soluble polyquinolines with tunable photophysical, redox, and electroluminescent properties. *Macromolecules* 2005;38:9539-47.

[8] Kondakova ME, Deaton JC, Pawlik TD, Giesen DJ, Kondakov DY, Young RH, et al. Highly efficient fluorescent-phosphorescent triplet-harvesting hybrid organic light-emitting diodes. *J Appl Phys* 2010;107:014515-014515-13.

[9] (a) Wang KY, Chen C, Liu JF, Wang Q, Chang J, Zhu HJ, et al. Novel

multifunctional organic semiconductor materials based on 4,8-substituted 1,5-naphthyridine: synthesis, single crystal structures, opto-electrical properties and quantum chemistry calculation. *Biomol Chem* 2012;10:6693-704; (b) Zhu TH, He GK, Chang J, Zhao DD, Zhu XL, Zhu HJ. The synthesis, photophysical and electrochemical properties of a series of novel 3,8,13-substituted triindole derivatives. *Dyes Pigm* 2012;95:679-88.

[10] (a) Axel DB. Density-functional thermochemistry. III. The role of exact exchange. *J Chem Phys* 1993;98:5648-5652; (b) Lee C, Yang W, Parr RG. Development of the Colle-Salvetti correlation-energy formula into a functional of the electron density. *Phys Rev B* 1988;37:785-789.

[11] (a) Clark T, Chandrasekhar J, Spitznagel GW, Schleyer PvR. Efficient diffuse function-augmented basis sets for anion calculations. III. The 3-21 + G basis set for first-row elements, lithium to fluorine. *J Comput Chem* 1983;4:294-301; (b) Francl MM, Pietro WJ, Hehre WJ, Binkley JS, Gordon MS, DeFrees DJ, et al. Self-consistent molecular orbital methods. XXIII. A polarizationtype basis set for second-row elements. *J Chem Phys* 1982;77:3654-3665; (c) Gill PMW, Johnson BG, Pople JA, Frisch MJ. The performance of the Becke-Lee-Yang-Parr (B-LYP) density-functional theory with various basis sets. *Chem Phys Lett* 1992;197:499-505; (d) Krishnan R, Binkley JS, Seeger R, Pople JA. Self-consistent molecular orbital methods. A basis set for correlated wave functions. *J Chem Phys* 1980;72:650-654.

[12] Frisch MJ, Trucks GW, Schlegel HB, Scuseria GE, Robb MA, Cheeseman JR, et al. *Gaussian 09, Revision B. 01*, Gaussian, Inc. Wallingford CT; 2010.

- [13] Eisch JJ. Aza-Aromatic Substitution. I. The selective bromination of the quinoline nucleus. *J Org Chem* 1962;27:1318-23.
- [14] Naito T. Polarization of aromatic heterocyclic compounds. LXXV. Nitration of quinoline 1-oxide having substituents in their benzene ring. *Yakugaku Zasshi* 1948;68:209-10.
- [15] (a) Loones KT, Maes BU, Dommissie RA. Synthesis of pyrido[2',1':2,3]imidazo[4,5-*b*]quinoline and pyrido[1',2':1,2]imidazo[4,5-*b*]quinoline and their benzo and aza analogs via tandem catalysis. *Tetrahedron* 2007;63:8954-61; (b) Huang S, Garbaccio RM, Fraley ME, Steen J, Kreatsoulas C, Hartman G. Development of 6-substituted indolylquinolinones as potent chek1 kinase inhibitors. *Bioorg Med Chem Lett* 2006;16:5907-12; (c) Klosterman JK, Linden A, Siegel JS. Synthesis of aryl-substitute 2-pyridyl-1,10-phenanthrolines; a series of oriented terpyridine analogues. *Org Biomol Chem* 2008;6:2755-2764.
- [16] Inglis SR, Stojkoski C, Branson KM, Cawthray JF, Fritz D, Wiadrowski E, et al. Identification and specificity studies of small-molecule ligands for SH3 protein domains. *J Med Chem* 2004;47:5405-17.
- [17] Gollner A, Koutentis PA. Two-step total syntheses of canthin-6-one alkaloids: new one-pot sequential Pd-catalyzed Suzuki-Miyaura coupling and Cu-catalyzed amidation reaction. *Org Lett* 2010;12:1352-5.
- [18] Couturier M, Le T. Safe and practical large-scale synthesis of 2-aminoquinoline-6-carboxylic acid benzyl ester. *Org Process Res Dev* 2006;10:534-8.
- [19] Kubota Y, Hara H, Tanaka S, Funabiki K, Matsui M. Synthesis and fluorescence

properties of novel pyrazine_boron complexes bearing a β -iminoketone ligand. *Org Lett* 2011;24:6545-7.

[20] (a) Wang B, Yu FB, Li P, Sun XF, Han KL. A BODIPY fluorescence probe modulated by selenoxide spirocyclization reaction for peroxyxynitrite detection and imaging in living cells. *Dyes Pigm* 2013;96:383-90; (b) Boens N, Leen V, Dehaen W. Fluorescent indicators based on BODIPY. *Chem Soc Rev* 2012;41:1130-72; (c) Silva AP, Gunaratne HQ, Gunnlaugsson T, Huxley AJ, McCoy CP, Rademacher JT, et al. Signaling recognition events with fluorescent sensors and switches. *Chem Rev* 1997;97:1515-66; (d) Baruah M, Qin W, Flors C, Hofkens J, Vallée R, Beljonne D, et al. Solvent and pH dependent fluorescent properties of a dimethylaminostyryl borondipyrromethene dye in solution. *J Phys Chem A* 2006;110:5998-6009.

[21] Suzuki K, Kobayashi A, Kaneko S, Takehira K, Yoshihara T, Ishida H, et al. Reevaluation of absolute luminescence quantum yields of standard solutions using a spectrometer with an integrating sphere and a back-thinned CCD detector. *Phys Chem Chem Phys* 2009;11:9850-60.

[22] Kasumov VT, Medjidov AA, Yayli N, Zeren Y. Spectroscopic and electrochemical characterization of di-*tert*-butylated sterically hindered Schiff bases and their phenoxyl radicals. *Spectrochimica Acta Part A* 2004;60:3037-47.

[23] Ulrich G, Ziessel R, Haefele A. A general synthetic route to 3,5-substituted boron dipyrromethenes: applications and properties. *J Org Chem* 2012;77:4298-4311.

[24] Wu CI, Lin CT, Chen YH, Chen MH. Electronic structures and electron-injection mechanisms of cesium-carbonate-incorporated cathode structures for organic light-emitting devices. *Appl Phys Lett* 2006;88:152104-1-3.

Tables

Table 1. Thermal Properties ^a of **B1-B6**.

Complex	T_m (°C)	T_g (°C)
B1	257	—
B2	> 400	—
B3	—	363
B4	> 400	—
B5	357	187
B6	—	278

^a DSC scans of **B1-B6** recorded under nitrogen during the second heating cycle at a scan rate of 10 °C min⁻¹.

Table 2. Optical properties of **B1-B6** in CH₂Cl₂ solution and in solid-state.

Complex	$\lambda_{\max}^{\text{abs}}$ (nm) ^a		ϵ_{\max} (10 ⁴ M ⁻¹ cm ⁻¹)	$\lambda_{\max}^{\text{em}}$ (nm) ^b		E_g^{opt} (eV) ^c	Stokes shift (nm)		τ_F (ns)	Φ_{PL} ^d	
	CH ₂ Cl ₂	Solid-state		CH ₂ Cl ₂	Solid-state		CH ₂ Cl ₂	Solid-state			
B1	453	446	5.6	521	530	2.67	2.40	3	55	3.57	0.93
B2	456	444	6.9	517	499	2.66	2.34	4	58	2.59	0.71
B3	451	457	7.0	518	515	2.70	2.37	2	57	3.14	0.63
B4	455	447	8.2	522	552	2.65	2.38	5	105	2.93	0.47

B5	457	430	6.5	522	518	2.64	2.32	6	88	3.00	0.69
B6	471	449	2.5	527	597	2.45	2.03	56	148	3.16	0.01

^a Recorded in 1×10^{-5} M CH_2Cl_2 solution at r.t. ^b Recorded in 10^{-7} M CH_2Cl_2 solution of at r.t. ^c Optical band gaps determined from the absorption edge of absorption spectra.

^d Determined in CH_2Cl_2 using 9,10-diphenylanthracene ($\Phi_{\text{PL}} = 0.97$ in cyclohexane) as standard at r.t.

Table 3. DFT calculation results of HOMO/LUMO energy levels.

Complex	LUMO (eV)	HOMO (eV)	$E_{\text{g}}^{\text{cal}}$ (eV) ^a
B1	-2.06	-5.74	3.68
B2	-2.01	-5.56	3.64
B3	-2.34	-6.04	3.70
B4	-2.70	-6.26	3.56
B5	-2.23	-5.59	3.36
B6	-2.00	-5.17	3.17

^a Carried out at the B3LYP/6-31G(D) level of theory.

Table 4. Electrochemical properties of the **B1-B6** ^a.

Complex	$E_{\text{red}}^{\text{peak}}$ (V)	$E_{\text{ox}}^{\text{peak}}$ (V)	$E_{\text{ox}}^{\text{onset}}$ (V)	HOMO (eV) ^b	LUMO (eV) ^c
B1	-0.46	0.70, 1.07, 1.63	0.51	-5.32	-2.65
B2	—	1.07	0.85	-5.61	-2.95

B3	-0.72	0.72	0.53	-5.33	-2.63
B4	-0.79	0.75	0.55	-5.35	-2.70
B5	—	0.91	0.73	-5.53	-2.89
B6	—	0.66, 0.58	0.47	-5.28	-2.83

^a Potentials determined by cyclic voltammetry in deoxygenated solution of CH₃CN/CH₂Cl₂ (7:3 v/v), containing 0.1 M TBAP, at a concentration of 10⁻³ M, at r.t. Potentials were standardized with ferrocene-ferrocenium (Fc/Fc⁺) couple as internal reference vs Ag/AgNO₃. Scan rate 100 mV/s. Working electrode: Pt, counter electrode: Pt wire, reference electrode: Ag/AgNO₃. ^b E_{HOMO} (eV) = -e($E_{\text{onset}}^{\text{ox}}$ + 4.8). ^c E_{LUMO} (eV) = -e(E_{HOMO} - $E_{\text{g}}^{\text{opt}}$).

Scheme and Figure captions:

Fig. 1. Normalized absorption spectra in CH_2Cl_2 (1×10^{-5} M) and emission spectra of **B1-B6** in CH_2Cl_2 (1×10^{-7} M).

Fig. 2. Normalized absorption (a) and emission spectra (b) of **B1-B6** in solid state.

Fig. 3. The optimized geometries and the molecular orbital surfaces of the HOMOs and LUMOs for **B1-B6** obtained at the B3LYP/6-31G level.

Fig. 4. Normalized emission spectra of **B6** in different solvents. The excitation wavelength was 440 nm.

Fig. 5. Cyclic voltammograms of **B1-B6** in $\text{CH}_3\text{CN}/\text{CH}_2\text{Cl}_2$ (7:3 v/v) (10^{-3} M) with working electrode: Pt, counter electrode: Pt wire, reference electrode: Ag/AgNO₃.

Scheme 1. Structures of BODIPY, aza-BODIPY derivatives and aza-BODIQU.

Scheme 2. Synthetic routes of complexes **B1-B6**.

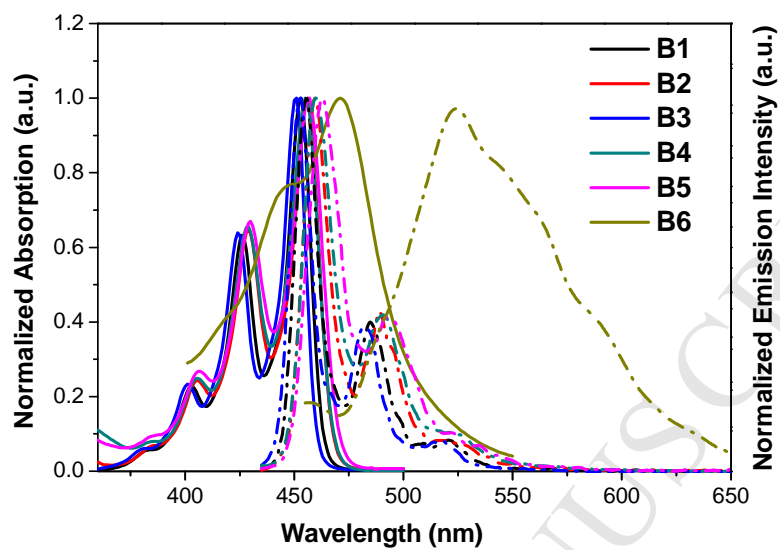


Fig. 1. Normalized absorption spectra in CH_2Cl_2 (1×10^{-5} M) and emission spectra of **B1-B6** in CH_2Cl_2 (1×10^{-7} M).

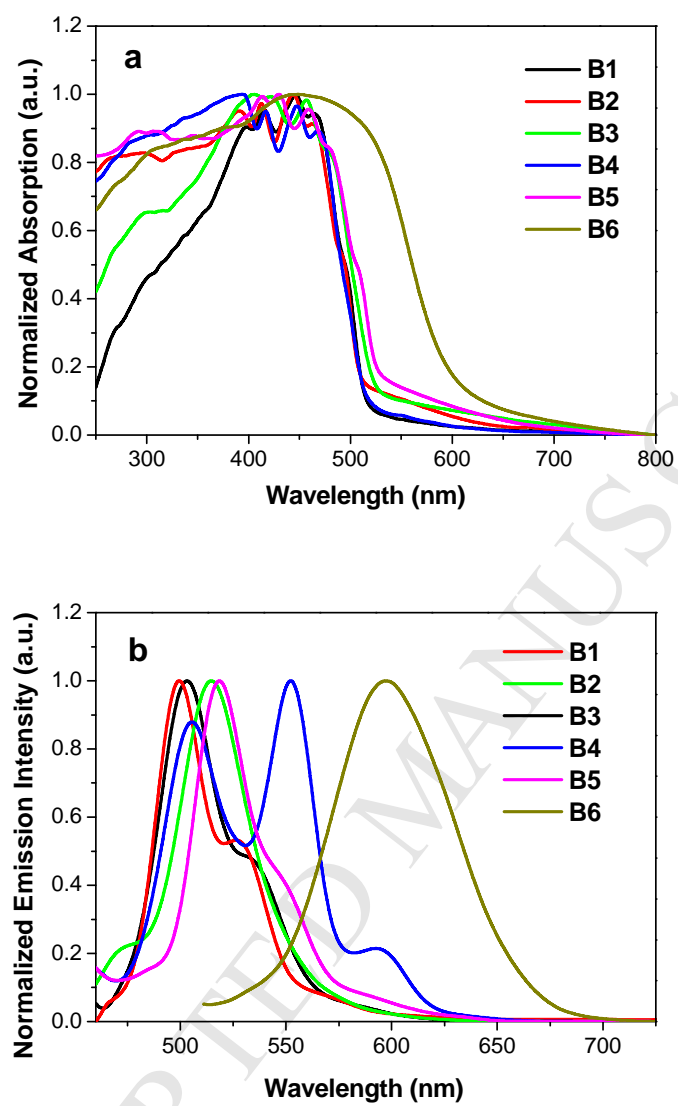


Fig. 2. Normalized absorption (a) and emission spectra (b) of **B1-B6** in solid state.

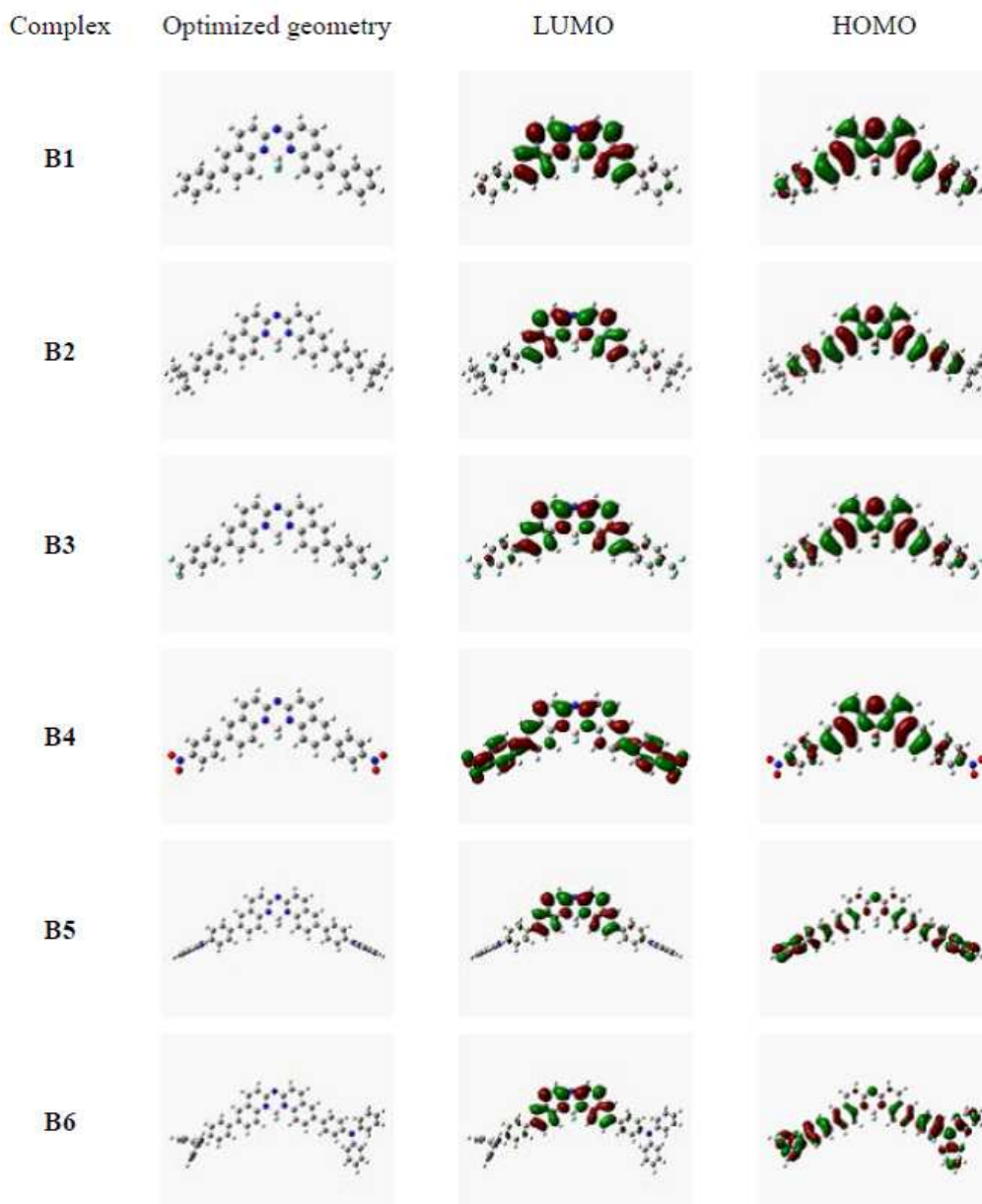


Fig. 3. The optimized geometries and the molecular orbital surfaces of the HOMOs and LUMOs for **B1-B6** obtained at the B3LYP/6-31G level.

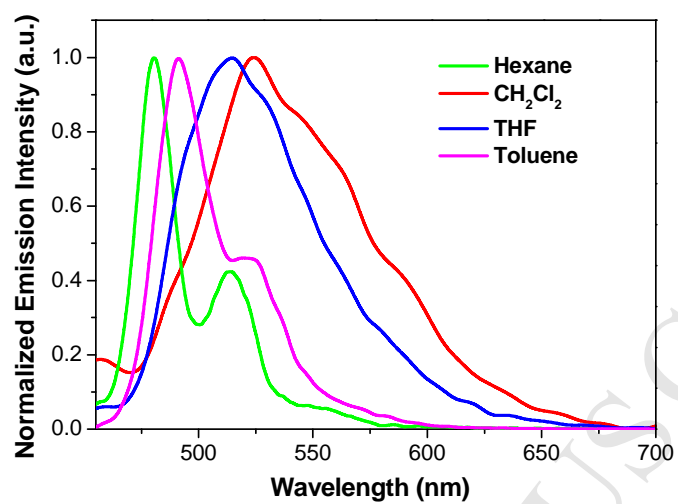


Fig. 4. Normalized emission spectra of **B6** in different solvents. The excitation wavelength was 440 nm.

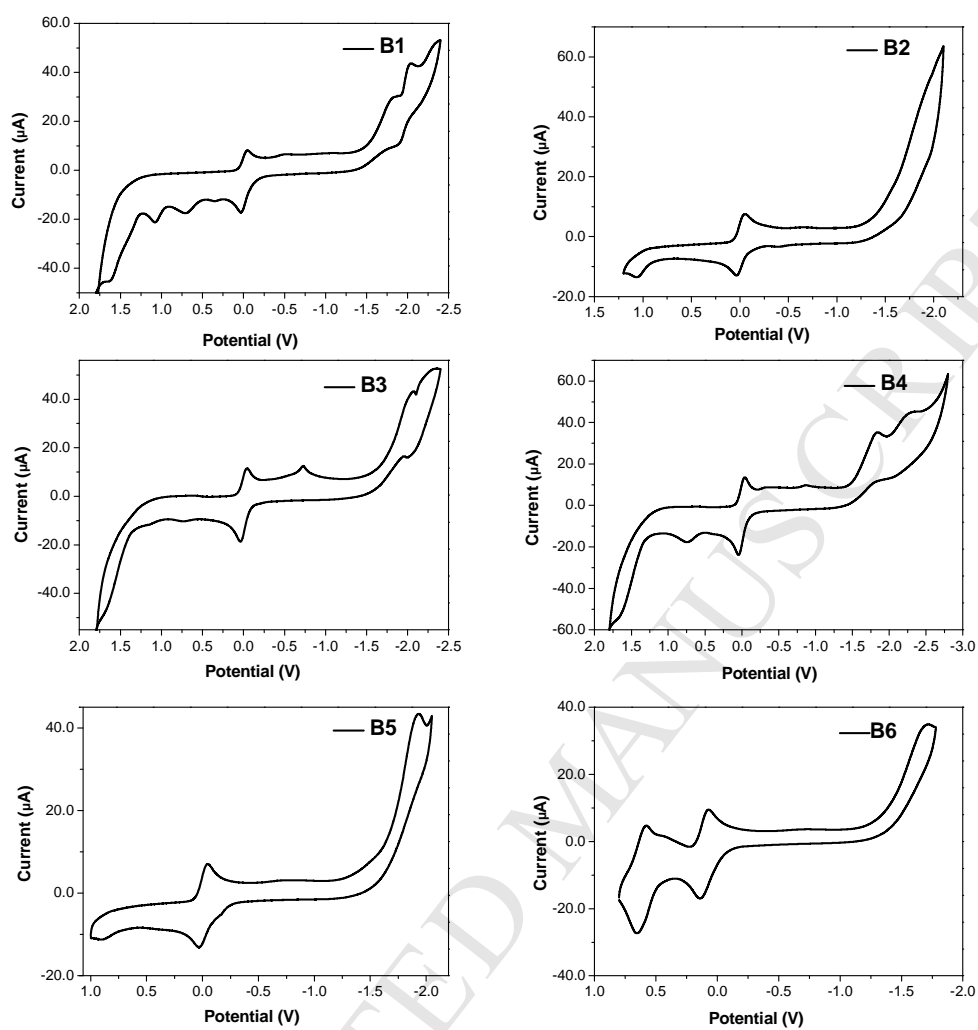
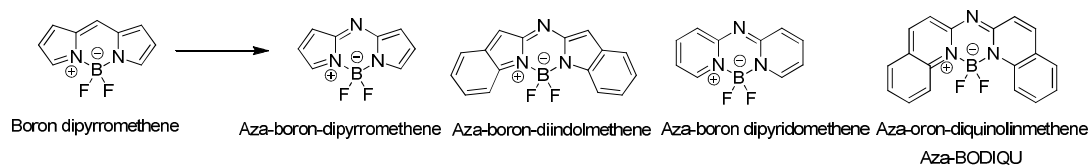
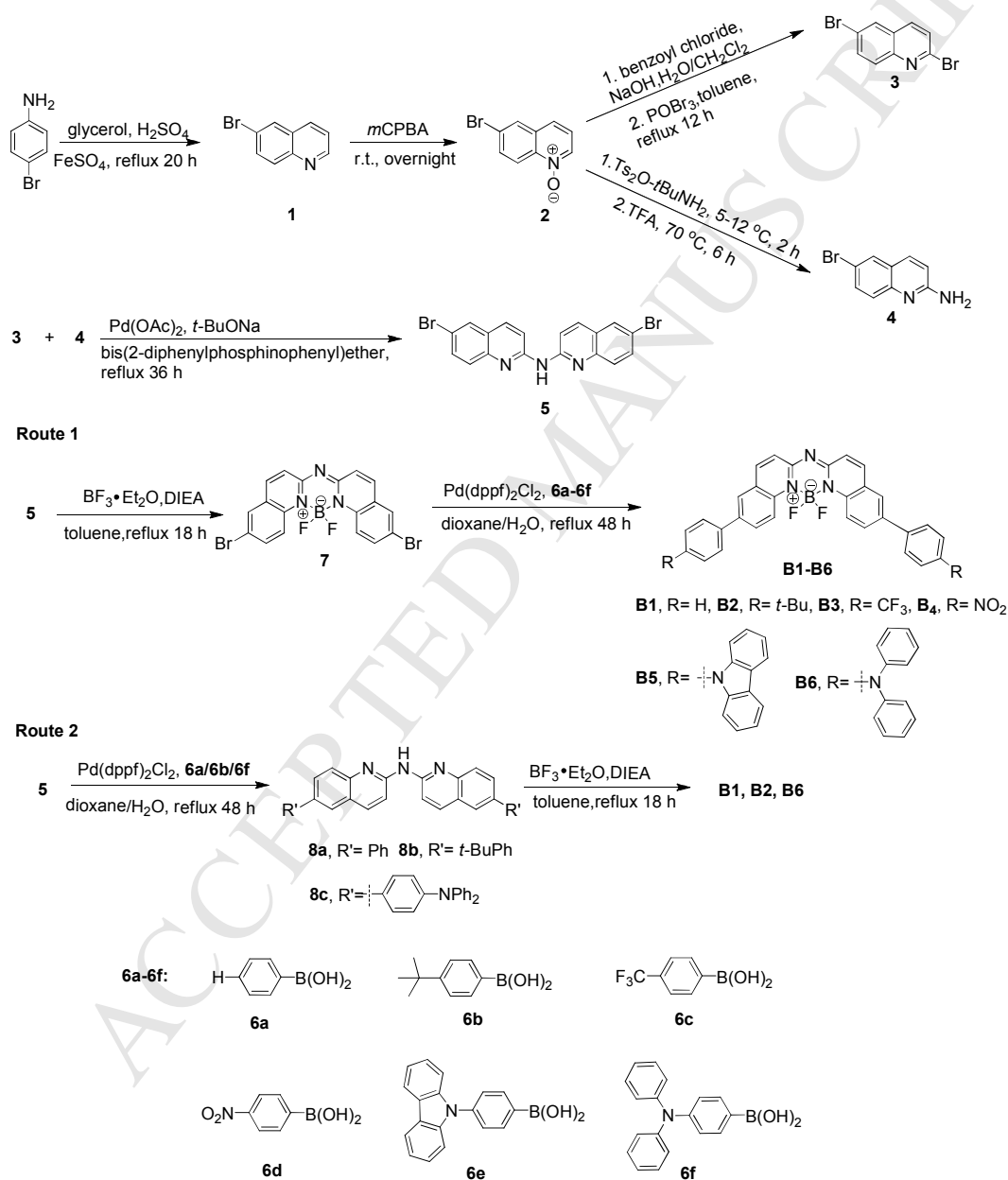


Fig. 5. Cyclic voltammograms of **B1-B6** in $\text{CH}_3\text{CN}/\text{CH}_2\text{Cl}_2$ (7:3 v/v) (10^{-3} M) with working electrode: Pt, counter electrode: Pt wire, reference electrode: Ag/AgNO_3 .



Scheme 1. Structures of BODIPY, aza-BODIPY derivatives and aza-BODIQU.

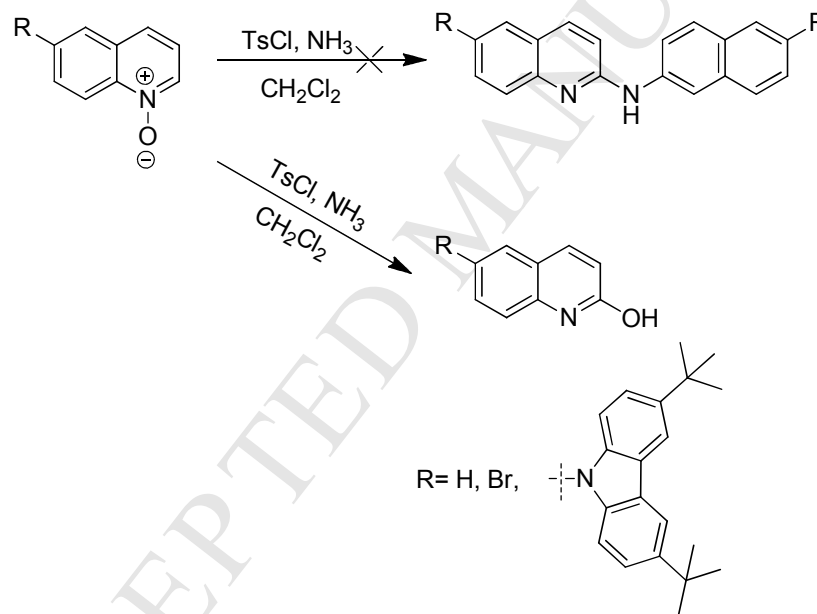


Scheme 2. Synthetic routes of complexes **B1-B6**.

Supporting Information

Synthesis, photophysical and electrochemical properties of
aza-boron-diquinomethene complexes

Danfeng Wang ^a, Rui Liu ^a, Chen Chen ^a, Shifan Wang ^a, Jin Chang ^b, Chunhui Wu ^a,
Hongjun Zhu ^{a*}, Eric R. Waclawik ^b



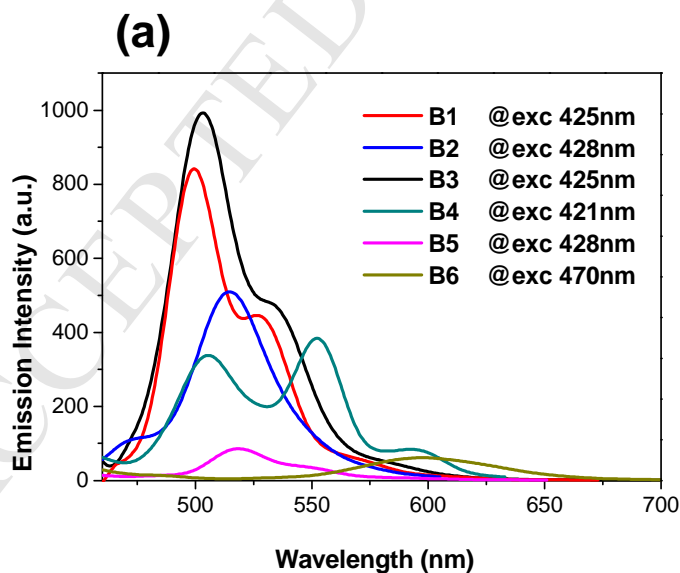
Scheme S1. Synthetic route of diquinolinamines.

Characterization

2-Hydroxyquinoline. Yellow solid, the yield was 56.7%, m.p. 198-200 °C. ¹H NMR (400 MHz, CDCl₃) δ (ppm): 12.09 (s, 1H), 7.82 (d, *J* = 9.5 Hz, 1H), 7.49-7.59 (m, 2H), 7.42 (d, *J* = 8.2 Hz, 1H), 7.19-7.25 (m, 1H), 6.72 (d, *J* = 9.5 Hz, 1H).

6-Bromoquinolin-2-ol. Yellow solid, the yield was 74.0%, m.p. 276-278 °C. ^1H NMR (400 MHz, CDCl_3) δ (ppm): 11.86 (s, 1H), 7.92 (d, $J = 1.7$ Hz, 1H), 7.87 (d, $J = 9.6$ Hz, 1H), 7.64 (dd, $J_1 = 8.8$ Hz, $J_2 = 1.7$ Hz, 1H), 7.24 (d, $J = 8.8$ Hz, 1H), 6.55 (d, $J = 9.6$ Hz, 1H).

6-(3,6-Di-tert-butyl-9H-carbazol-9-yl)quinolin-2-ol. Pale yellow solid, the yield was 65.3%, m.p. >300 °C. ^1H NMR (400 MHz, CDCl_3) δ (ppm): 11.99 (s, 1H), 8.29 (d, $J = 1.7$ Hz, 2H), 8.01 (d, $J = 9.6$ Hz, 1H), 7.95 (d, $J = 2.2$ Hz, 1H), 7.73 (dd, $J_1 = 8.7$ Hz, $J_2 = 2.3$ Hz, 1H), 7.54 (d, $J = 8.7$ Hz, 1H), 7.47 (dd, $J_1 = 8.7$ Hz, $J_2 = 1.9$ Hz, 1H), 7.29 (d, $J = 8.6$ Hz, 2H), 1.42 (s, 18H).



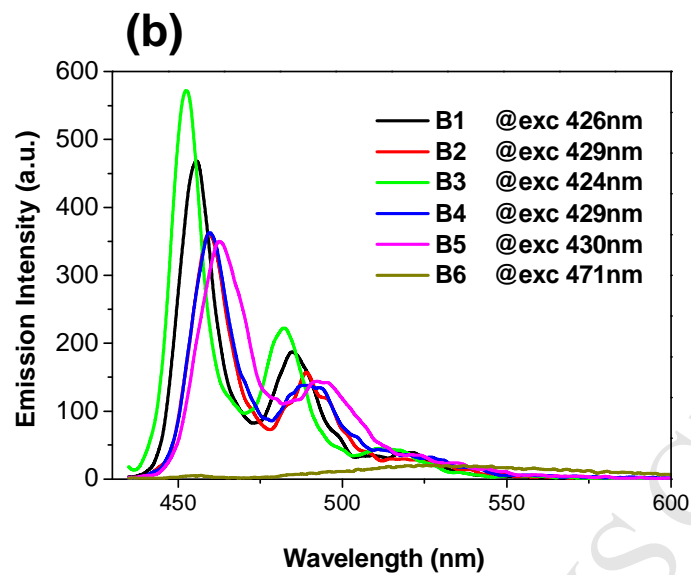


Fig. S1. Emission spectra of **B1-B6** in the solid state (a) and in CH_2Cl_2 (1×10^{-7} M)

(b).

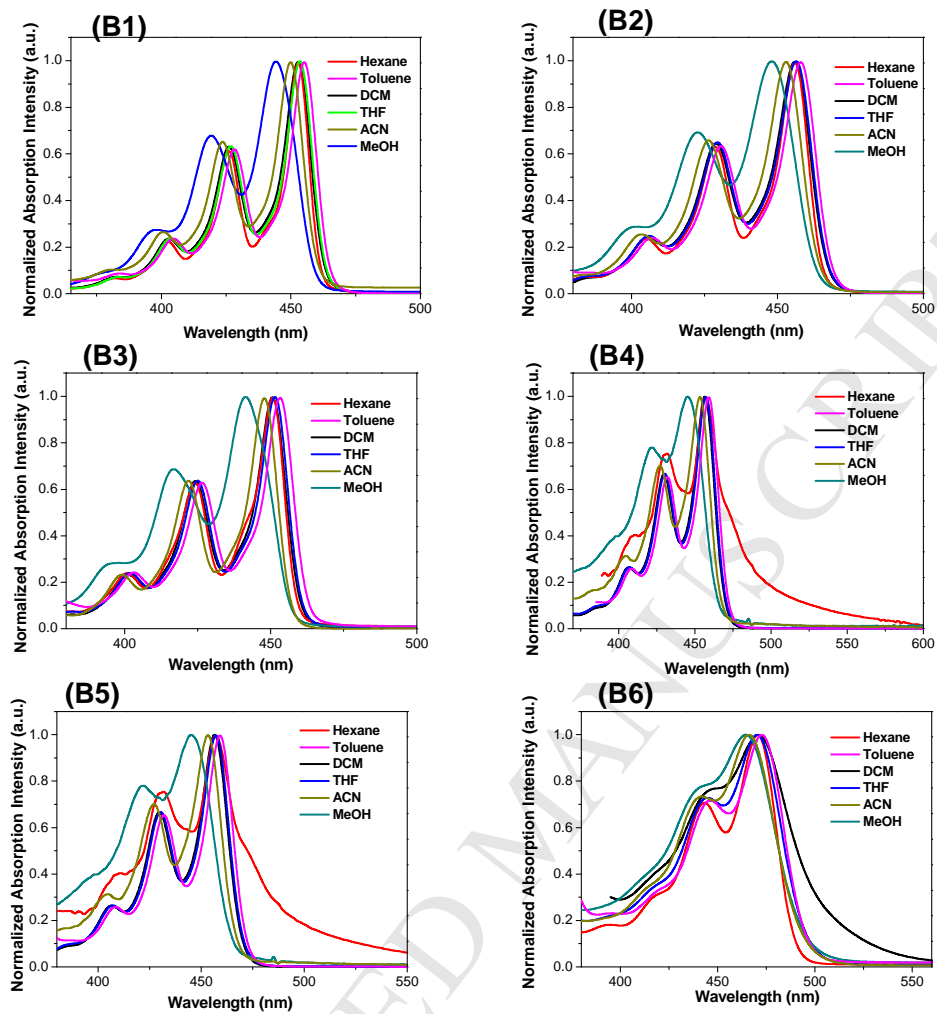


Fig. S2. Normalized absorption spectra of **B1-B6** in different solvents (1×10^{-5} M).

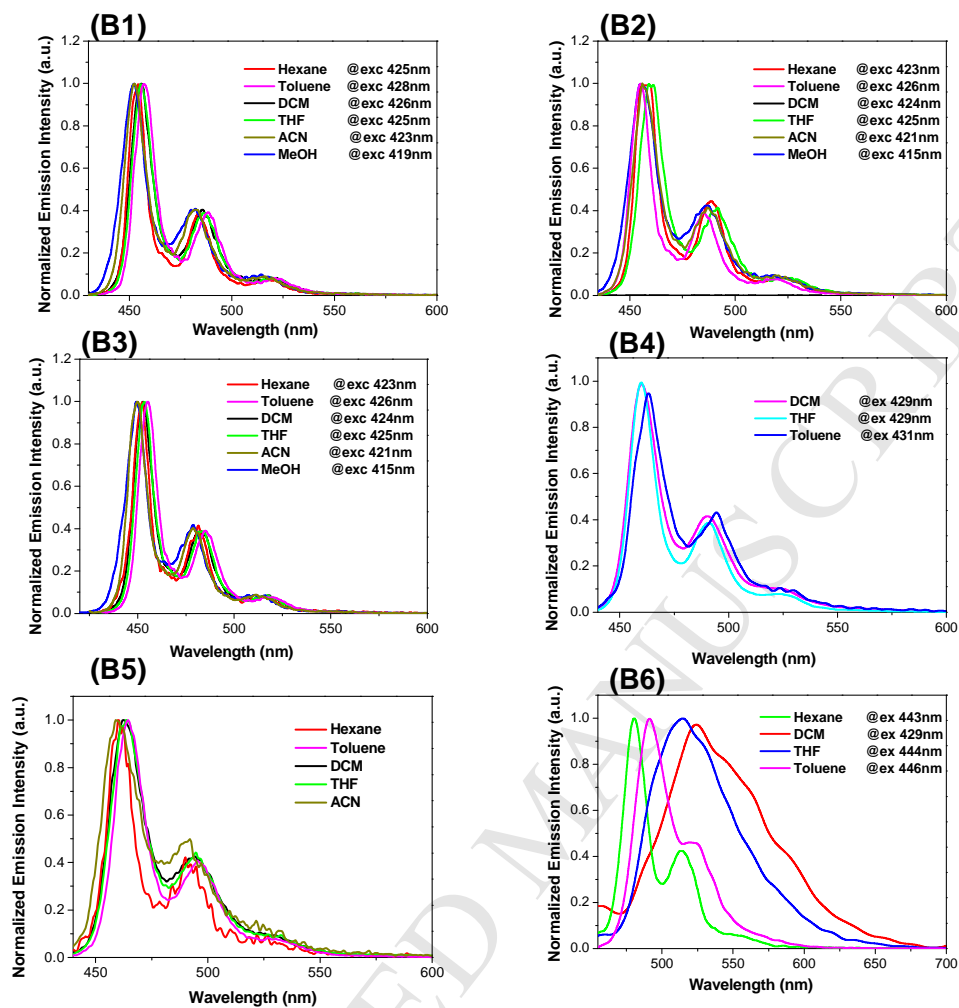


Fig. S3. Normalized emission spectra of **B1-B6** in different solvents (1×10^{-5} M).

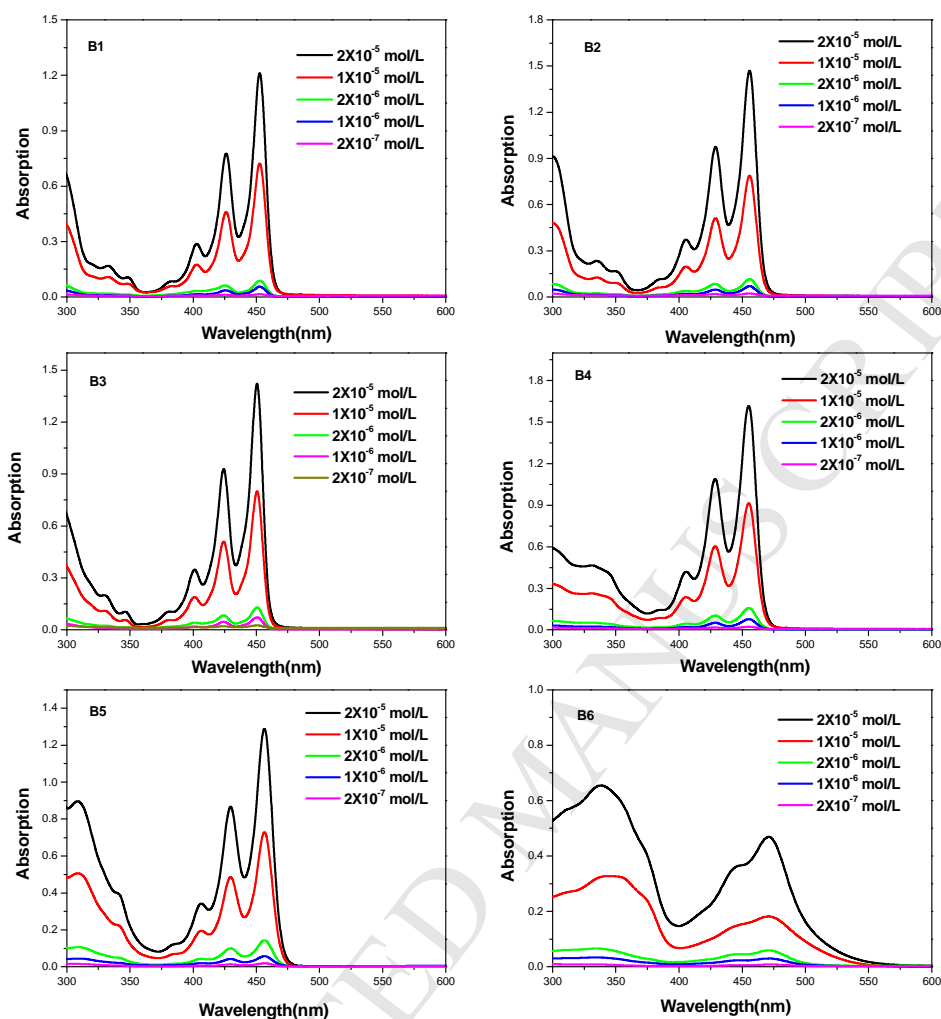


Fig. S4. Absorption spectra of **B1-B6** in CH_2Cl_2 of different concentrations (2×10^{-5} - 2×10^{-7} M).

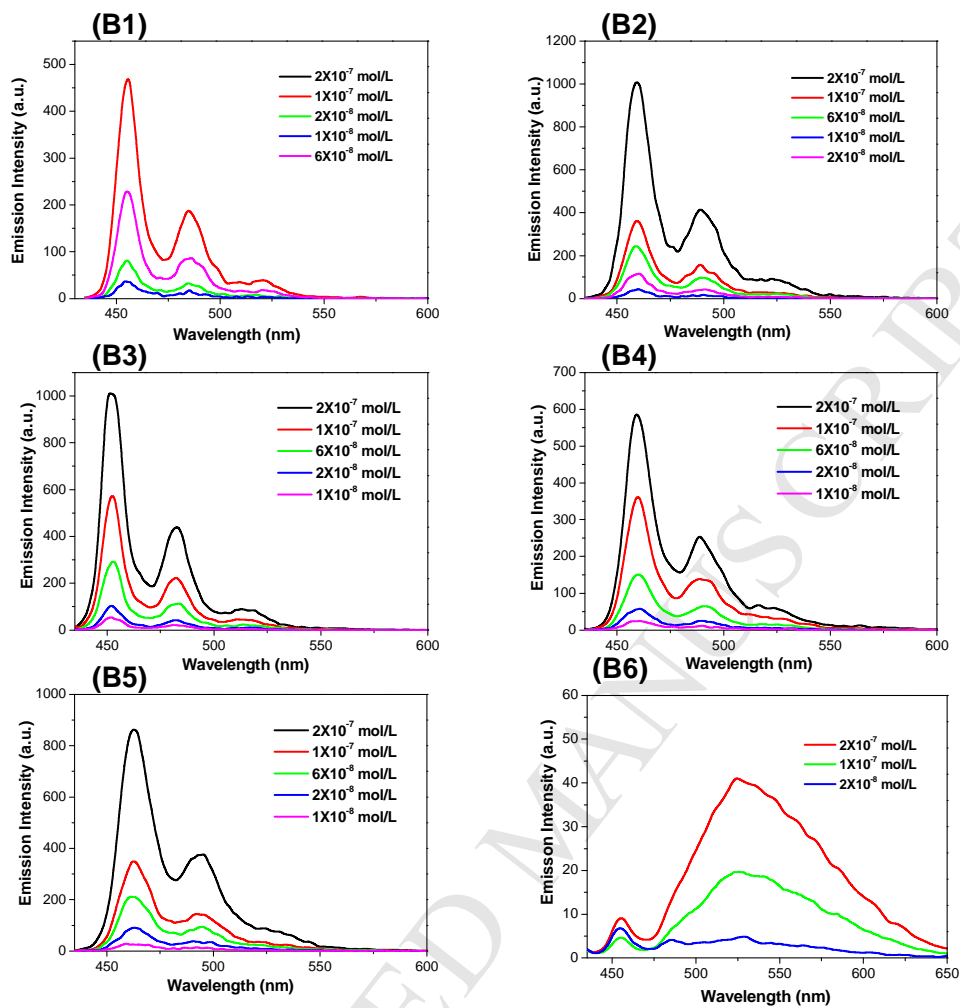


Fig. S5. Emission spectra of **B1-B6** in CH_2Cl_2 of different concentrations (1×10^{-8} - 2×10^{-7} M).

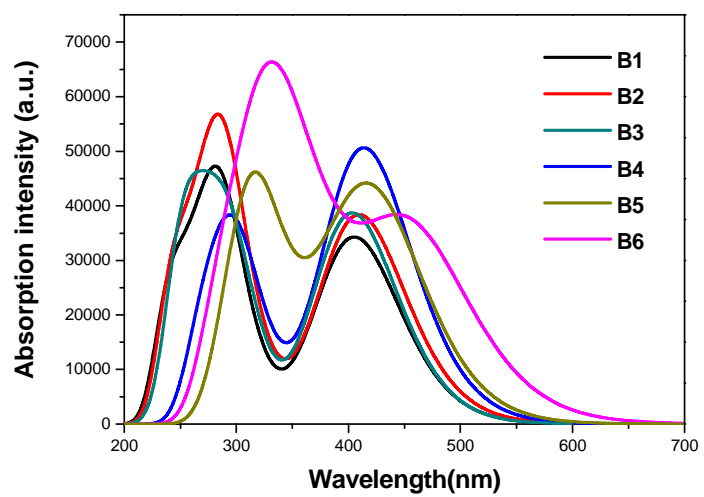


Fig. S6. Calculated absorption spectra of **B1-B6**.

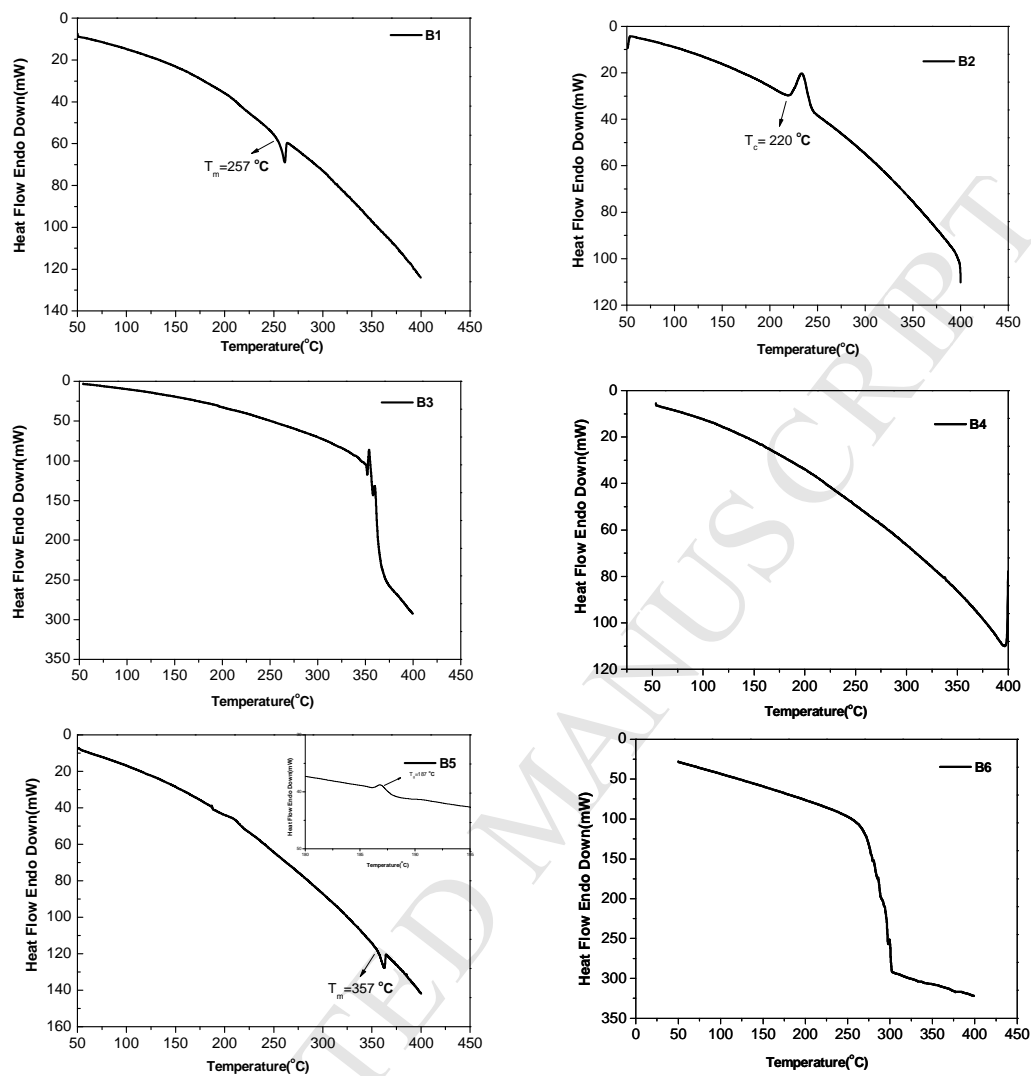
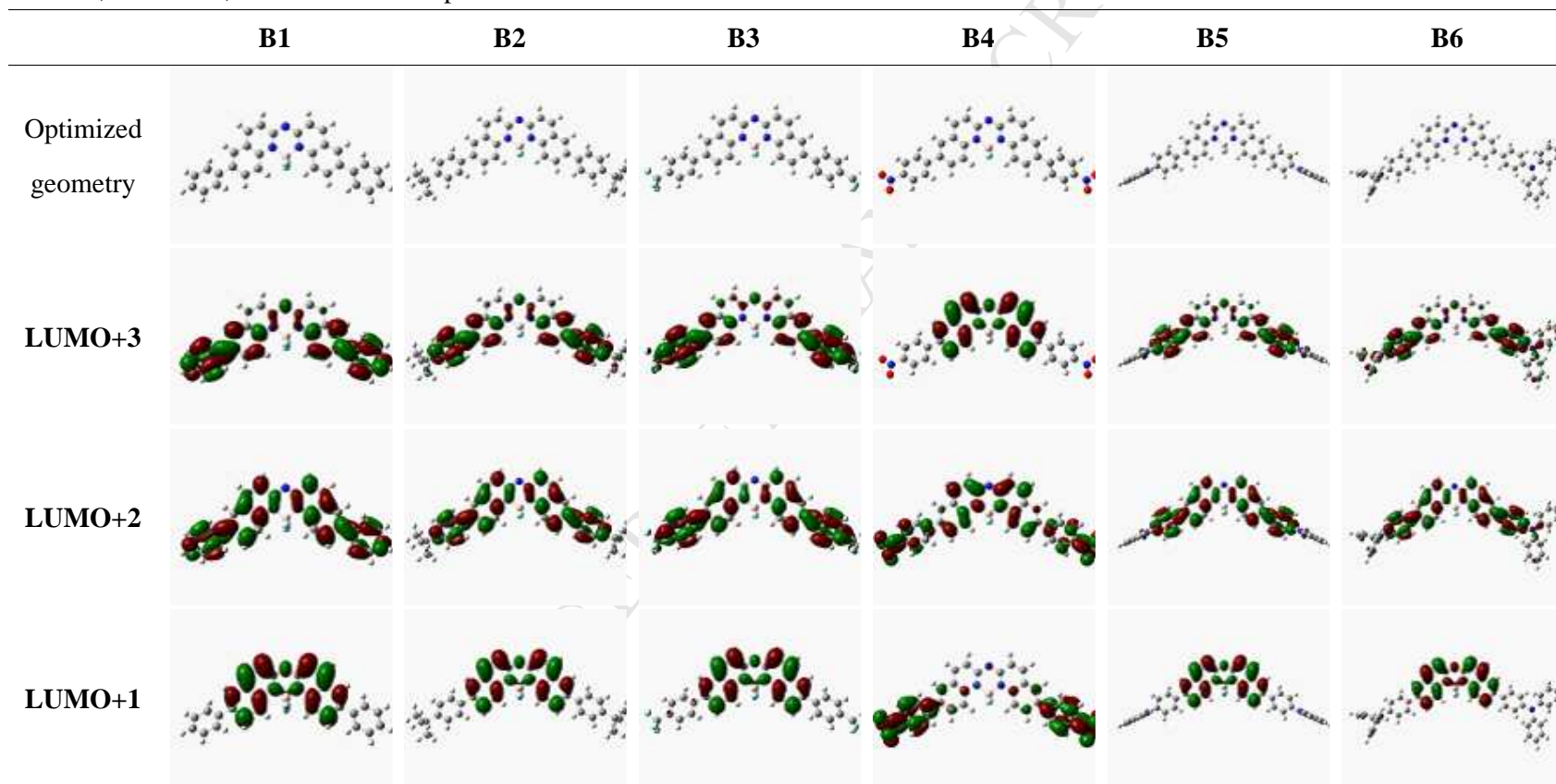


Fig. S7. DSC thermograms of **B1-B6** under a nitrogen atmosphere at a heating rate of 10 °C min^{-1} .

Table S1. Contour plots of the occupied molecular orbital HOMO, HOMO-1, HOMO-2, HOMO-3 and unoccupied molecular orbital LUMO, LUMO+1, LUMO+2, LUMO+3 for complexes **B1-B6**.



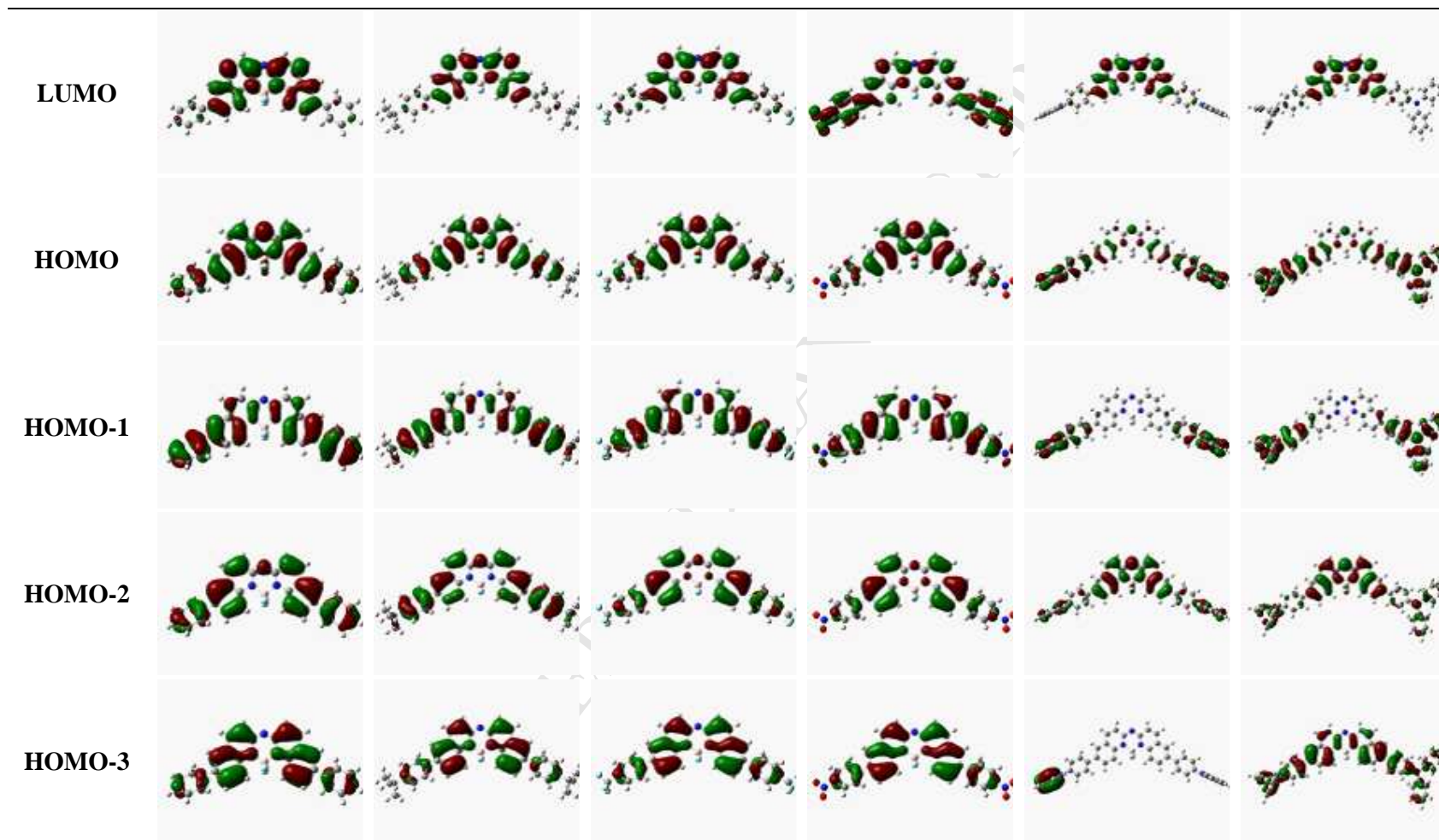


Table S2. TDDFT-derived molecular orbital energies (eV) of **B1-B6**

	B1	B2	B3	B4	B5	B6
LUMO+3	-0.71	-0.63	-1.25	-1.72	-1.01	-0.75
LUMO+2	-0.83	-0.76	-1.28	-2.27	-1.09	-0.83
LUMO+1	-1.27	-1.21	-1.53	-2.46	-1.42	-1.20
LUMO	-2.06	-2.01	-2.34	-2.70	-2.23	-2.00
HOMO	-5.74	-5.65	-6.04	-6.26	-5.59	-5.17
HOMO-1	-6.46	-6.28	-6.85	-7.11	-5.65	-5.25
HOMO-2	-6.78	-6.65	-7.10	-7.33	-6.01	-5.85
HOMO-3	-7.07	-6.98	-7.37	-7.61	-6.05	-6.60

Table S3. Excitation energies (eV), wavelengths (nm), oscillator strengths, dominant contributing configuration, and the associated configuration coefficient of five low-lying electronic states of complex **B1-B6** obtained at the PBE1PBE level of theory.

B1

S_n	Excitation energy		f	Active orbital pair of dominant configuration	Configuration coefficient
	eV	nm			
1	3.06	406	0.8443	HOMO \rightarrow LUMO	0.70
2	3.74	332	0.0016	HOMO \rightarrow LUMO+1	0.59
3	3.83	324	0.1027	HOMO-1 \rightarrow LUMO	0.59
4	4.02	309	0.0085	HOMO-2 \rightarrow LUMO	0.64
5	4.28	290	0.7693	HOMO \rightarrow LUMO+2	0.63

B2

S_n	Excitation energy		f	Active orbital pair of dominant configuration	Configuration coefficient
	eV	nm			
1	3.02	410	0.9434	HOMO \rightarrow LUMO	0.70
2	3.69	336	0.0130	HOMO-1 \rightarrow LUMO	0.56
3	3.76	330	0.0962	HOMO \rightarrow LUMO+1	0.55
4	3.98	311	0.0172	HOMO-2 \rightarrow LUMO	0.64
5	4.24	293	0.9028	HOMO \rightarrow LUMO+2	0.61

B3

S_n	Excitation energy		f	Active orbital pair of dominant configuration	Configuration coefficient
	eV	nm			
1	3.07	404	0.9543	HOMO \rightarrow LUMO	0.70
2	3.77	329	0.0045	HOMO \rightarrow LUMO+2	0.63
3	3.93	315	0.1085	HOMO \rightarrow LUMO+2	0.63

4	4.02	308	0.0186	HOMO-2 → LUMO	0.55
5	4.21	295	0.6200	HOMO → LUMO+2	0.56

B4

S_n	Excitation energy		f	Active orbital pair of dominant configuration	Configuration coefficient
	eV	nm			
1	2.99	415	1.2272	HOMO → LUMO	0.69
2	3.41	363	0.0601	HOMO → LUMO+1	0.70
3	3.51	353	0.0160	HOMO → LUMO+2	0.68
4	3.78	328	0.0029	HOMO → LUMO+3	0.58
5	3.81	325	0.0015	HOMO-9 → LUMO+1	0.47

B5

S_n	Excitation energy		f	Active orbital pair of dominant configuration	Configuration coefficient
	eV	nm			
1	2.91	427	0.8912	HOMO → LUMO	0.65
2	3.08	403	0.0324	HOMO-1 → LUMO	0.70
3	3.27	379	0.3230	HOMO-2 → LUMO	0.65
4	3.53	351	0.0000	HOMO-3 → LUMO	0.70
5	3.52	351	0.0000	HOMO-4 → LUMO+1	0.70

B6

S_n	Excitation energy		f	Active orbital pair of dominant configuration	Configuration coefficient
	eV	nm			
1	2.71	458	0.8111	HOMO → LUMO	0.68
2	2.88	431	0.0541	HOMO-1 → LUMO	0.70
3	3.30	376	0.5716	HOMO-2 → LUMO	0.68
4	3.49	356	0.0002	HOMO → LUMO+1	0.67
5	3.61	344	0.4758	HOMO-1 → LUMO+1	0.60